theoretical and applied ergonomics

MDPI

Article

A Paired Mixed-Effects Analysis of Lumbar Shear and Compression Forces in Manual Lifting

Davide Piovesan * and Xiaoxu Ji

Biomedical Industrial and Systems Engineering Department, Gannon University, Erie, PA 16541, USA; ji001@gannon.edu

* Correspondence: piovesan001@gannon.edu; Tel.: +1-814-871-7221

Abstract

The Revised NIOSH Lifting Equation and the screening practices built around it interpret lumbar injury risk primarily through axial compression, yet anterior–posterior shear is associated with injury at loads below established compressive thresholds. L4 and L5 as are henceforth defined as the 4th and 5th lumbar vertebrae Using a harmonized database of 106 peak-loading lifting postures reconstructed through digital human modeling across five studies, we developed parallel families of linear mixed-effects regression models for L4/L5 compression and shear that shared identical predictor sets and matched random-effects structures, isolating biomechanical differences from differences in statistical specification. Load magnitude and horizontal hand reach acted as universal drivers of both outcomes—positive, highly significant, and stable across model reduction—although compression was several times more sensitive in absolute terms. The two components diverged in their posture sensitivities: knee flexion was significant only for shear, whereas trunk flexion, shoulder flexion, and vertical hand position acted predominantly on compression. Critically, no predictor significant in both families reversed sign, indicating that posture selectively modulates two independently sourced quantities—the moment arm of the supported mass, which governs compression, and the orientation of the lumbar segment, which governs shear—rather than redistributing a single conserved spinal reaction. Between-subject variability consistently exceeded between-task variability and persisted across model reduction, identifying individual lifting strategy as a structural determinant of spinal exposure. Among the 102 observations below the 3.4 kN compression criterion, 11 (10.8%) exceeded the lower 700 N shear reference, although none exceeded the upper 1000 N reference. Together these findings give a quantitative rationale for regarding compression-only assessment as structurally incomplete and support a multidimensional, posture-aware approach to ergonomic risk evaluation.

Keywords: NIOSH Lifting Equation; spinal shear force; manual material handling; ergonomic risk assessment; biomechanical modeling; mixed-effects regression; occupational safety; lifting biomechanics; predictive modeling

Check for updates

Academic Editor: Philippe Gorce

Received: 30 May 2026
Revised: 19 August 2026
Accepted: 7 September 2026
Published: 24 September 2026

Copyright: © 2026 by the authors. Licensee MDPI, Basel, Switzerland. This article is an open access article distributed under the terms and conditions of the Creative Commons Attribution (CC BY) license.

1. Introduction

Low-back disorders (LBDs) remain among the most prevalent and economically significant work-related musculoskeletal conditions [1–4], contributing to reduced productivity, chronic disability, and substantial healthcare and compensation costs across industrial sectors [5,6]. Manual material handling, particularly lifting, has long been recognized as

a major contributor to lumbar injury risk, motivating decades of ergonomic and biomechanical research aimed at understanding how external load, lifting geometry, and body posture influence spinal mechanical demand. Among the most widely adopted assessment approaches, the Revised NIOSH Lifting Equation (RNLE) [7] provides a practical framework for evaluating lifting tasks in occupational settings by combining epidemiological and biomechanical evidence into a series of task-based multipliers [8–10].

Although the RNLE incorporates multiple descriptors of lifting geometry and task organization, including load magnitude, horizontal and vertical hand location, coupling quality, asymmetry, and lifting frequency, its biomechanical rationale is historically anchored to lumbar compressive loading thresholds at the lumbosacral joint [11–14]. Consequently, both industrial screening practices and a large portion of ergonomic research have traditionally interpreted spinal loading primarily through the lens of axial compression, often treating compressive force as the dominant mechanical indicator of lifting-related injury risk [15,16].

More recent biomechanical and clinical evidence, however, suggests that anterior–posterior lumbar shear loading represents a partially independent pathway of spinal tissue stress with important implications for injury development [17–21]. Elevated shear forces have been associated with mechanisms involved in disc herniation, vertebral slippage (spondylolisthesis), and facet joint degeneration, in some cases at loading magnitudes substantially below established compressive safety thresholds (700–1000 N [9]). Computational simulations and experimental investigations increasingly indicate that compression and shear do not necessarily increase proportionally under equivalent lifting conditions. Changes in trunk orientation, lower-extremity posture, or object location may substantially amplify one loading mode while producing comparatively limited changes in the other. This mechanical dissociation suggests that ergonomic frameworks relying exclusively on compression-oriented interpretations may overlook important dimensions of lumbar loading and therefore incompletely characterize spinal injury risk [9,22].

At the same time, direct comparison between compression and shear loading mechanisms has remained difficult because of a persistent methodological divide within ergonomics research. Field practitioners typically rely on simplified observational tools that are broadly accessible but biomechanically limited, whereas research-oriented investigations employ advanced inverse- or forward-dynamics digital human models capable of estimating internal spinal forces with substantially greater fidelity. While these simulation-based approaches provide detailed insight into spinal mechanics, they generally require motion capture systems, specialized software environments, and computational expertise that limit routine workplace implementation [23–25].

To address this gap, we previously developed two independent mixed-effects statistical modeling frameworks derived from a common harmonized database of lifting postures reconstructed through digital human modeling (N = 106 peak-loading observations). One study focused specifically on estimating L4/L5 compressive loading [26], whereas the second examined predictors of L4/L5 anterior–posterior shear loading [27]. Both investigations demonstrated that high-fidelity biomechanical outputs generated through digital human modeling could be statistically approximated using ergonomically accessible task descriptors and posture variables through linear mixed-effects regression approaches implemented in MATLAB (version R2023a, MathWorks, Natick, MA, USA) [16,28,29].

However, despite the development of these independent predictive frameworks, the biomechanical relationship between compression and shear loading under matched lifting conditions remains insufficiently understood. The prior studies evaluated each loading component separately and therefore did not examine how equivalent ergonomic conditions redistribute internal mechanical demand between compression- and shear-dominant

pathways. Consequently, the operational and biomechanical implications of these model families relative to one another have remained unresolved. A direct paired comparison is necessary to determine whether posture, load geometry, and subject-specific movement strategies influence compression and shear through shared or fundamentally distinct mechanical mechanisms.

Accordingly, the present work provides an integrated paired-model comparison of lumbar compression and shear forces developed from a shared multi-study digital human modeling database. By aligning matched fixed-effects, random-intercept, and random-slope model structures across both loading outcomes, the study examines how load magnitude, hand position, sex, and joint kinematics reshape the internal loading environment of the lumbar spine under equivalent task conditions. Particular emphasis is placed on identifying where the determinants of compression and shear converge, where they diverge, and how posture functions as a dynamic load redistribution strategy rather than as a uniform amplifier of spinal demand. Through this parallel statistical framework, the present study moves beyond single-metric ergonomic interpretation and advances a multidimensional perspective of spinal loading relevant to next-generation ergonomic assessment systems. Ultimately, the proposed framework provides a biomechanically informed conceptual foundation for future posture-aware and sensor-driven ergonomic technologies—including computer-vision pose estimation and sparse wearable sensing systems—that may enable clinically informed spinal risk assessment directly within industrial environments [29–35].

2. Materials and Methods

2.1. Comparative Modeling Framework and Task-Space Harmonization

The present study builds upon two previously developed mixed-effects regression frameworks derived from a shared biomechanical simulation database: one modeling lumbar compression loading [26] and the other modeling lumbar anterior–posterior shear loading [27]. Rather than generating additional biomechanical simulations, the objective of the current work is to directly compare how equivalent ergonomic and postural variables influence spinal loading through these two independently derived regression architectures. Accordingly, the methodological workflow consisted of three sequential stages: (1) biomechanical estimation of spinal loading through digital human modeling, (2) extraction and harmonization of task- and posture-related predictors from the simulated lifting tasks, and (3) paired comparison of the resulting compression- and shear-based mixed-effects regression models.

The underlying biomechanical database was constructed from five previously completed lifting investigations representing diverse applications including industrial materials handling [36], healthcare patient transfer tasks [37], virtual-reality lifting environments [30], brewery ergonomics workflows [31], and digital human model validation scenarios [38]. Across these studies, lifting tasks intentionally spanned a broad reachable workspace relative to the support base defined by foot position. The retained lifting configurations therefore included deep-squat floor retrievals, elevated placements, asymmetric patient-transfer maneuvers, extended forward reaches, and heavy industrial lifting conditions involving loads ranging from 5 kg to 72 kg. To characterize the breadth of the pooled task space, descriptive statistics for all predictor variables and loading outcomes are reported in Table 1. The dataset spans a wide range of hand locations, and postural configurations, providing substantial variability for both compression and shear model development. In particular, the workspace includes horizontal hand positions from 35 to 95 cm, and vertical hand positions from 20 to 126 cm, encompassing both near-body and extended-reach lifting conditions.

Table 1. Descriptive statistics of the pooled lifting dataset used for compression and shear model development.

Variable	Mean	SD	Min	Max
Load (kg)	16.76	12.82	5.0	72.0
Horizontal Distance, H (cm)	44.98	10.42	35.0	95.0
Vertical Distance, V (cm)	89.08	28.54	20.0	126.0
Reach Distance, D (cm)	55.18	33.56	0.0	120.0
Trunk Flexion (deg)	−3.82	13.69	−39.90	43.48
Hip Flexion (deg)	−0.58	43.37	−115.10	101.60
Knee Flexion (deg)	−3.72	28.39	−105.80	78.20
Shoulder Flexion (deg)	49.87	26.80	−2.80	114.50
Elbow Flexion (deg)	−24.80	34.14	−106.10	16.60
Shoulder Abduction/Adduction (deg)	−21.83	29.20	−84.10	26.30
L4/L5 Compression Force (N)	2762.29	1263.65	635.90	6830.75
L4/L5 Shear Force (N)	579.94	314.79	57.90	1614.98

Notably, mean compression loading (2762 N) was approximately 4.8 times greater than mean anterior–posterior shear loading (580 N), a difference that should be considered when comparing coefficient magnitudes and variance components between the two model families.

As a result, the pooled dataset captured substantial variability in horizontal hand distance, vertical hand position, trunk inclination, lower-extremity posture, and external moment-arm geometry relative to the feet. Some tasks positioned the load close to the body while requiring large hip and knee flexion, whereas others involved extended anterior reaches combined with comparatively upright lower-extremity configurations. Additional lifting conditions combined elevated hand placement with forward trunk inclination or asymmetric support postures. This broad spatial and postural variability was biomechanically important because lumbar compression and anterior–posterior shear do not necessarily scale proportionally across equivalent reachable workspaces. Instead, the spatial relationship between the hands, trunk, pelvis, and support base can redistribute spinal loading differently across the two relative directional components.

In all contributing studies, full-body kinematic recordings were reconstructed within the Siemens JACK (v9.0, Siemens software, Plano, TX, USA) digital human modeling environment, where lumbar joint reaction forces were estimated using inverse-kinematic biomechanical procedures. Only postures corresponding to peak mechanical demand within each lifting task were retained for analysis, as these configurations represented the biomechanically critical instants used to construct both the compression and shear regression frameworks. For each retained posture, both lumbar compression and anterior–posterior shear forces were extracted at the same biomechanically critical instant, ensuring direct comparability between the two loading outcomes.

Following biomechanical reconstruction, each lifting observation was reformulated into a standardized ergonomic representation using NIOSH-derived task descriptors and posture variables extracted from the simulations. These predictors included load magnitude, horizontal and vertical hand position, coupling quality, and joint-angle descriptors for the hip, knee, trunk, shoulder, and elbow. Coupling quality was harmonized across the source datasets using the NIOSH coupling definition. The binary variable *Coupling_Good* was coded as 1 when the hand–object interface satisfied the NIOSH criteria for good coupling and as 0 for all other coupling conditions. The same operational criterion was applied across all five source studies. This is the same operational definition used in the previously published outcome-specific compression and shear analyses [26,27]. Because

this harmonized variable distinguishes only good from poor coupling, it does not represent finer differences in handle geometry, surface friction, object shape, grip configuration, or intermediate coupling conditions. Because identical variable definitions, biomechanical reconstruction procedures, and harmonization strategies were applied across all retained datasets, the resulting predictor space remained fully consistent between the compression and shear modeling frameworks.

The present analysis therefore compares two parallel regression families derived from identical lifting tasks, shared biomechanical simulations, and equivalent ergonomic predictor spaces, differing only in the spinal loading outcome used as the dependent variable. This alignment enables direct evaluation of how equivalent task geometry and postural organization influence spinal loading differently across compression- and shear-dominant mechanical pathways. Because equivalent variable definitions and harmonization procedures were applied to the two outcomes, the paired framework reduces the possibility that differences between the compression and shear coefficients arise merely from inconsistent parameter definitions. Residual heterogeneity associated with the objectives, environments, and acquisition procedures of the source studies cannot be eliminated completely. Study-level heterogeneity was evaluated in the published outcome-specific model-development analyses through specifications containing StudyID, SubjectID, and TaskID random intercepts [26,27], and the present study should be interpreted as a comparative synthesis of those established model families.

2.2. Statistical Modeling Framework

The primary objective of the statistical analysis was to identify how standard NIOSH lifting parameters and detailed posture descriptors influence lumbar shear and compression forces and to determine whether their effects differ meaningfully between the two load components. To accomplish this, we constructed parallel families of mixed-effects regression models that shared identical predictor sets and closely matched random-effects structures. This approach ensured that differences in estimated coefficients arise from the underlying biomechanics of shear and compression, rather than from disparities in statistical specification [39].

The general model structure can be expressed as

$$Y_{ijk} = \beta_0 + \sum_{p=1}^{P} \beta_p X_{pijk} + u_i + v_j + \varepsilon_{ijk}$$

where

- Y_{ijk} is either lumbar shear force or compression force for observation k, subject i, and task j;
- β_0 is the fixed intercept;
- X_p represents the fixed predictors;
- β_p are fixed-effect coefficients;
- u_i is the random subject effect;
- v_j is the random task effect;
- ε is residual error.

All models treated either anterior–posterior shear force or axial compression force at the L4/L5 segment as the dependent variable. Predictor variables were selected to represent the fundamental contributors to spinal mechanical loading and included load magnitude, horizontal and vertical hand location, coupling quality, and sex, together with joint-angle descriptors capturing hip, knee, trunk, shoulder, and elbow configuration at the moment of peak demand. Each predictor was treated as a fixed effect

to estimate its population-level association with spinal loading across the full pooled dataset (see Table A1).

Because the lifting trials originated from multiple studies and involved repeated measurements from individual participants performing multiple tasks, hierarchical structure was present in the data. To reflect this dependency and to isolate population-level effects from person- or task-specific variation, mixed-effects models incorporated random intercepts for both SubjectID and TaskID where appropriate. These random terms allowed the regression to account for inherent differences in baseline loading across individuals and across distinct lifting tasks within a study. In the more complex model variants, random slopes for load magnitude and horizontal hand location were added at the subject level to capture individual variability in how sensitive lumbar forces were to increases in load weight or forward reach. Such variability is expected given natural differences in anthropometry, lifting strategy, and neuromuscular control. The random-slope formulations was

$$Y_{ijk} = \beta_0 + (\beta_{Load} + u_{Load,i})Load_{ijk} + (\beta_H + u_{H,i})H_{ijk} + \sum \beta_p X_{pijk} + u_i + v_j + \varepsilon_{ijk}$$

where

$$u_{Load,i} \sim N\left(0, \sigma^2_{Load}\right)$$

$$u_{H,i} \sim N\left(0, \sigma^2_{H}\right)$$

represent subject-specific sensitivities.

All models were estimated using restricted maximum likelihood to provide stable variance-component estimates, particularly in models containing random slopes. Coefficients were interpreted in their natural units (Newtons per degree, Newtons per centimeter, or Newtons per kilogram), allowing direct biomechanical interpretation of each parameter. Model diagnostics were conducted to confirm appropriate residual behavior and absence of collinearity patterns that could bias coefficient estimation.

Through this parallel modeling strategy, the analysis isolates the degree to which load magnitude, hand location, posture, and anthropometric factors exert similar or divergent influences on lumbar shear and compression forces. The resulting comparison provides a rigorous statistical foundation for understanding the mechanical pathways by which ergonomic variables shape spinal loading during lifting tasks.

Model selection was structured to allow direct pairing of shear- and compression-based models at each level of statistical complexity. Fixed-effects-only models served as baseline formulations that quantify pure predictor effects without accounting for repeated-measures structure. Random-intercept models provided a more realistic representation of the hierarchical design while maintaining interpretability of the population-level coefficients. Random-slope models allowed the analysis to incorporate inter-individual differences in response to the most mechanically influential variables. By creating shear and compression models with parallel structures at each of these tiers, we established a controlled framework for comparing how strongly and in what direction each predictor influences the two outcomes. For the characteristic of each model, see Table 2.

Table 2. Overview of the mixed-effects model specifications evaluated during the model-development process. Each model is described in terms of the predictors it included, the random-effects structure applied, and the number of fixed coefficients, random coefficients, and covariance parameters that resulted from its design.

Model	Fixed Effects Included	Random-Effects Structure	Number of Fixed Parameters	Number of Grouping-Level Random-Effect Coefficients
S0	Full model: Load, H, V, Sex, Coupling, HipFlex, KneeFlex, TrunkFlex, ShoulderFlex, ElbowFlex, ShAbdAdd	None (no random intercepts)	12	0
S2	Same as S0	SubjectID + TaskID random intercepts	12	42
S4	Same as S0	Random slopes for Load_kg and H_cm (SubjectID) + TaskID intercept	12	144
S9	Removed Coupling + TrunkFlex + Sh_AbdAdd	SubjectID + TaskID random intercepts	9	42
S10	Further reduced: remove ShoulderFlex	SubjectID + TaskID random intercepts	8	42
S11	Same as 10	SubjectID random intercept	8	36
C0	Load, H, V, Sex, Coupling, Hip, Knee, Trunk, Shoulder, Elbow, Sh_AbdAdd	None (fixed-effects only; residual error term only)	12	0
C2	Same fixed effects as C0	Subject intercept; Task intercept	12	42
C4	Same fixed effects as C0	Subject intercept + random slopes for Load and H; Task intercept; additional covariance terms	12	114
C8	All fixed effects except Coupling	Subject intercept; Task intercept	11	42
C10	Load, H, V, Sex, Hip, Knee, Trunk, Shoulder, Elbow	Subject intercept; Task intercept	10	42
C11	Load, H, V, Sex, Hip, Trunk, Shoulder, Elbow	Subject intercept; Task intercept	9	42

2.3. Paired Model Selection and Pruning Logic

The independent exploratory analyses for L4/L5 compression [26] and anterior–posterior (A–P) shear [27] originally evaluated separate 12-model structural pathways to solve their respective load profiles. Those studies evaluated the influences of numerous parameters, including study-, subject-, and task-level random intercepts; intermediate and expanded subject-specific random-slope structures; systematic fixed-effect reduction; variance-component behavior; coefficient stability; and model-selection criteria. The present study does not reproduce those development analyses. Instead, it intentionally isolates a matched subset of six model pairs (12 specifications total) for direct cross-examination. Structurally matched milestones were selected from the two published model families to permit direct comparison of compression and shear under equivalent predictor specifica-

tions. Readers are referred to the precursor studies for the complete diagnostic results and outcome-specific model-selection rationale.

Rather than presenting a disjointed look at non-continuous mathematical steps, models were selected a priori based on their ability to capture identical, parallel milestones of statistical complexity, hierarchical variance partitioning, and targeted variable reduction. Models pertinent to the shear force will be denominated as $S_i \mid i \in W$, while models describing the compression force will be described as $C_i \mid i \in W$. The structural matching criteria for the retained pairs are explicitly defined as follows:

- The Deterministic Baselines (S_0 and C_0): Retained as fixed-effects-only reference models to establish baseline population-level performance without hierarchical clustering.
- The Random Intercepts (S_2 and C_2): Selected to represent the entry-level hierarchical architecture, allowing individual participant and task baseline shifts to be explicitly isolated while retaining the complete, unrestricted 12-parameter predictor block.
- The Random Slopes (S_4 and C_4): Chosen to evaluate maximum structural flexibility, allowing subject-specific sensitivities to the dominant mechanical drivers—load magnitude (Load_kg) and horizontal reach (H_cm)—to vary dynamically.
- The Parsimonious Pruned Subsets (S_8 *vs.* C_9, S_{10} *vs.* C_{10}, and S_{11} *vs.* C_{11}): Retained because they trace the exact convergence pathways where non-significant upper-extremity joint angles and task modifiers were systematically stripped away to maximize explanatory parsimony.

Because these specific milestones are mapped directly back to their parent investigations [26,27], the original model index numbers are strictly preserved to maintain algorithmic traceability across our research group's ongoing spinal safety paradigm.

Cross-outcome robustness testing was inherent in this model-development structure. Both outcome families began with the same complete predictor block, so variables ultimately retained in only one final model had already been evaluated in the other outcome family before reduction. In particular, C10 contains the complete C11 compression specification plus knee flexion, the posture variable retained uniquely in the final shear model. Conversely, the complete shear models included trunk and shoulder flexion, which were ultimately retained only for compression. The different final predictor sets therefore resulted from outcome-specific statistical support within a common initial predictor space rather than from the use of different candidate variables.

2.4. Comparative Coefficient Mapping and Sensitivity Interpretation

The objective of the present comparative analysis was not limited to evaluating predictive performance of the compression- and shear-based regression frameworks, but rather to examine how equivalent ergonomic and postural variables differentially influence spinal loading across the two mechanical pathways. Accordingly, the regression coefficients were interpreted as biomechanical sensitivity descriptors relating changes in task geometry and body posture to changes in lumbar loading magnitude.

Because both regression families were constructed from identical lifting tasks, shared biomechanical simulations, and equivalent predictor spaces, differences in coefficient magnitude, sign, and stability could be directly interpreted as differences in mechanical load redistribution behavior between lumbar compression and anterior–posterior shear. Larger absolute coefficient magnitudes indicated greater sensitivity of the spinal loading outcome to a given ergonomic or postural variable, whereas differences in coefficient direction reflected whether a variable increased or reduced loading within a particular mechanical pathway.

Particular emphasis was placed on evaluating how spatial relationships between the hands, trunk, pelvis, and support base altered the relative contribution of compression

and shear loading. Variables associated with horizontal hand displacement, vertical load position, trunk inclination, and lower-extremity posture were therefore examined comparatively to determine whether equivalent changes in reachable workspace geometry produced proportional or divergent loading responses across the two regression architectures.

In addition to fixed-effect coefficients, the hierarchical random-effects structure was interpreted biomechanically rather than solely statistically. Subject-level random intercepts and slopes were used to represent variability associated with individual lifting strategies, posture selection, and movement organization across equivalent tasks. Consequently, differences in variance structure between the compression and shear models were interpreted as evidence that subjects may redistribute spinal loading differently depending on task geometry and postural configuration.

The paired comparison therefore treated the regression frameworks as matched biomechanical sensitivity maps derived from the same lifting environment. Rather than focusing exclusively on predictive accuracy, the analysis examined how equivalent ergonomic variables propagate through the two regression structures to reveal distinct compression- and shear-oriented loading behaviors within the lumbar spine.

3. Results

3.1. Comparison of Model Architectures and Reduction Strategy

To evaluate whether lumbar compression and shear forces respond similarly to increasing model complexity, parallel families of mixed-effects regression models were developed for each outcome using matched predictor sets and comparable hierarchical structures (Table 2). The series ranged from fixed-effects-only formulations (S0, C0) to specifications incorporating subject- and task-level random intercepts (S2, C2), random slopes for the dominant predictors (S4, C4), and progressively reduced models (S9–S11, C8–C11). All coefficients reported in this section are drawn from Table A2 (and its graphic representation in Figure 1) and all p-values from Table A3. In Figure 1, non-significance of the coefficients can be identified if the 95% confidence interval contains 0.

The baseline models S0 and C0 contained the most comprehensive fixed-effects structure, with eleven predictors: load magnitude; horizontal and vertical hand location; sex; coupling quality; and joint-angle descriptors for the hip, knee, trunk, shoulder, and elbow, together with shoulder abduction/adduction. These models included no hierarchical structure beyond the residual error term and served as deterministic reference formulations.

Models S2 and C2 introduced random intercepts for subject and task while preserving the full predictor set. This structure allows baseline spinal loading to differ across individuals and lifting conditions without altering the assumed population-level relationships. Models S4 and C4 then added random slopes for load magnitude and horizontal reach at the subject level, the two predictors mechanically expected to dominate spinal loading and to vary most across individuals. The consequences of this added flexibility for model fit and variance partitioning are reported in Sections 3.2 and 3.4; the present section focuses on the behavior of the fixed-effect coefficients.

Adding the random intercepts left the dominant fixed effects largely intact but reshaped the smaller posture terms. Load, horizontal reach, sex, and hip flexion changed only modestly: shear load moved from 17.9 $\pm$ 3.1 N/kg (S0) to 19.3 $\pm$ 4.0 N/kg (S2), and compression load from 93.5 $\pm$ 13.3 N/kg (C0) to 101.3 $\pm$ 29.0 N/kg (C2), each remaining significant at $p < 0.001$ or better. The upper-extremity terms behaved differently. Shoulder flexion reversed sign once hierarchical structure was added, shifting from -1.0 N/deg (S0) to +0.7 N/deg (S2) in the shear models and from -3.7 N/deg (C0) to +4.8 N/deg (C2) in the compression models. For compression, elbow flexion moved from non-significant (-2.0 N/deg, $p = 0.39$, C0) to significant (-6.1 N/deg, $p = 0.004$, C2), while knee flexion

fell from 6.8 N/deg (p = 0.03, C0) to 3.4 N/deg and lost significance (p = 0.14, C2). This pattern—stable dominant predictors alongside unstable, sign-switching upper-extremity terms—motivated the variable removals described below, and indicates that the fixed-only estimates (S0, C0) should be interpreted with caution, since they absorb between-subject structure into the slope coefficients.

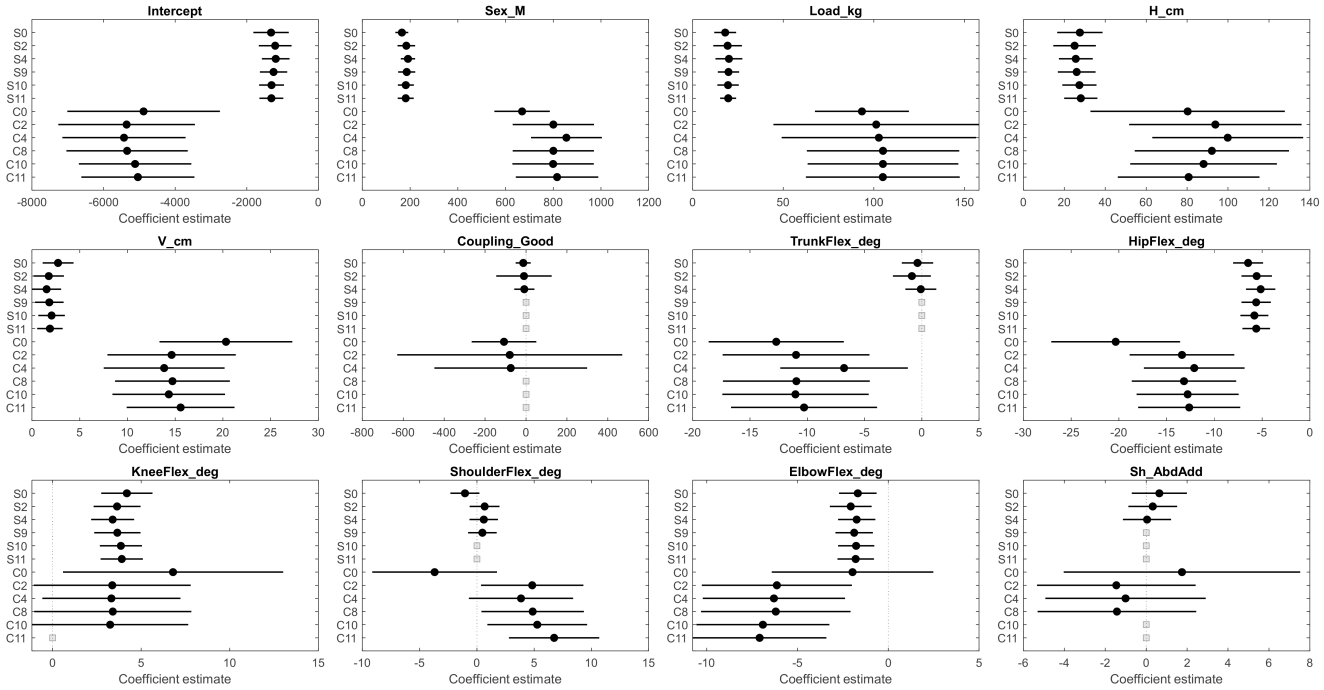


Figure 1. Regression Coefficients Forest Plot of fixed-effect regression coefficients across the shear (S) and compression (C) model families. Points represent estimated regression coefficients and horizontal bars represent 95% confidence intervals. The vertical reference line indicates a coefficient of zero; confidence intervals crossing zero indicate nonsignificant effects at the 0.05 level.

In the shear family, the three predictors that were non-significant in the random-intercept model were removed first. Coupling quality (p = 0.74, S2), trunk flexion (p = 0.31, S2), and shoulder abduction/adduction (p = 0.60, S2) were dropped together in S9, reducing the fixed structure from twelve to nine parameters. Shoulder flexion remained non-significant after this step (p = 0.45, S9) and was removed next in S10. The final shear model, S11, retained this eight-predictor set and removed the task-level intercept, leaving subject identity as the only grouping factor. Every predictor retained in the final shear model (S11) was significant: load (19.6 $\pm$ 2.3 N/kg, $p < 0.001$), horizontal reach (28.0 $\pm$ 4.1 N/cm, $p < 0.001$), sex (181.8 $\pm$ 17.1 N, $p < 0.001$), hip flexion (-5.6 ± 0.7 N/deg, $p < 0.001$), knee flexion (3.9 $\pm$ 0.6 N/deg, $p < 0.001$), and elbow flexion (-1.8 ± 0.5 N/deg, $p < 0.001$), with vertical position weaker but still significant (1.9 $\pm$ 0.7 N/cm, p = 0.007).

The compression family shed a different set of variables along a shorter path. Coupling quality was again non-significant ($p = 0.70$, C2) and was removed first in C8. Shoulder abduction/adduction followed ($p = 0.47$, C8) and was removed in C10. The final reduction occurred in C11, where knee flexion was removed. The C10-to-C11 comparison provides the cross-outcome robustness check requested here: C10 contained all predictors retained in C11 together with knee flexion, the posture variable retained uniquely in the final shear model. Although knee flexion was significant in the fixed-effects-only compression model, it lost significance after hierarchical structure was introduced and remained non-significant in the random-intercept compression models ($p = 0.14$, C2; 3.25 ± 2.25 N/deg, $p = 0.15$, C10). Its removal produced only modest changes in the remaining coefficient estimates.

Thus, knee flexion was not absent from the final compression model because it had not been tested; it was removed after repeated evaluation showed that its association was not robust to the hierarchical model structure.

The compression retained is equally informative. The final compression model, C11, included trunk flexion (-10.3 ± 3.3 N/deg, $p = 0.002$) and shoulder flexion (6.7 ± 2.0 N/deg, $p = 0.001$)—both non-significant for shear—alongside the shared core of load (105.0 ± 21.7 N/kg), horizontal reach (80.8 ± 17.7 N/cm), vertical position (15.6 ± 2.9 N/cm), sex (815.9 ± 88.3 N), hip flexion (-12.6 ± 2.7 N/deg), and elbow flexion (-7.1 ± 1.9 N/deg), each significant at $p < 0.001$. Unlike the final shear model, C11 also retained the task-level intercept (TaskID SD = 108.9 N).

This difference reflects the outcome-specific variance structures rather than an a priori assumption that task identity affects compression but not shear. In the reduced shear models, the TaskID standard deviation remained approximately 10–11 N and could be removed with minimal effect on model fit or the retained coefficients. In the compression family, the TaskID standard deviation remained approximately 106–109 N in the final reduced models, indicating a more persistent task-level contribution after the measured predictors had been included.

The reciprocal cross-outcome comparison was embedded in the shear pathway. Trunk and shoulder flexion, which were retained in the final compression model, were included in the complete hierarchical shear model. Trunk flexion was small and non-significant (-0.87 ± 0.84 N/deg, $p = 0.31$, S2), and shoulder flexion was likewise non-significant (0.67 ± 0.67 N/deg, $p = 0.31$, S2). Their removal from the reduced shear models therefore followed direct outcome-specific testing rather than an a priori decision to exclude compression-related variables.

The two pruning paths therefore converge on a shared core and diverge on the posture variables in a near mirror-image pattern. Both outcomes retained load magnitude, horizontal and vertical hand position, sex, hip flexion, and elbow flexion, and both discarded coupling quality and shoulder abduction/adduction. The difference lies in three posture angles. Knee flexion was significant for shear ($p < 0.001$, S11) but not compression ($p = 0.14$, C2), and survived only in the shear models. Trunk and shoulder flexion were significant for compression ($p = 0.002$ and $p = 0.001$, C11) but never approached significance for shear (both $p > 0.30$, S2), and survived only in the compression models. The hierarchical structure split along the same line: the final shear model retained variability only between subjects, whereas the final compression model retained both subject- and task-level variability. This symmetric divergence—knee-driven simplification for shear, trunk- and shoulder-driven retention for compression—indicates that the two loading components are governed by partly different posture determinants, and supports treating them as a paired comparison rather than collapsing them into a single spinal-load metric.

3.2. Model Performance and Selection

Model comparison was conducted within each outcome family, since information criteria computed on different dependent variables are not directly comparable; the higher absolute indices of the compression models reflect the larger scale of compressive loading rather than poorer fit. Within both families, accounting for hierarchical variability substantially improved fit relative to the fixed-effects-only formulations (Table 3). Across both outcomes, reductions in AIC, BIC, and deviance, together with increases in log likelihood, consistently favored mixed-effects specifications, indicating that a meaningful portion of spinal loading variability is attributable to subject- and task-specific effects beyond the fixed ergonomic descriptors.

Table 3. Summary of model performance indices.

Model	AIC	BIC	Log Likelihood	Deviance
S0	1153.3	1186.4	−563.65	1127.3
S2	1140.4	1178.5	−555.18	1110.4
S4	1115.7	1166.6	−537.87	1075.7
S9	1146.5	1177.4	−561.24	1122.5
S10	1145.8	1174.2	−561.91	1123.8
S11	1144.3	1170.1	−562.13	1124.3
C0	1427.3	1460.3	−700.64	1401.3
C2	1381.7	1419.9	−675.87	1351.7
C4	1370.5	1421.4	−665.26	1330.5
C8	1392.2	1427.9	−682.09	1364.2
C10	1393.9	1427.2	−683.95	1367.9
C11	1397.4	1428.3	−686.71	1373.4

Intermediate random-slope specifications, including subject-specific variation in the load coefficient alone, were evaluated in the published outcome-specific model-development studies [26,27]. Although these models improved some likelihood-based fit indices, they produced inflated variance components, unstable fixed-effect estimates, and covariance structures approaching singularity. The present paired analysis therefore retains the maximum random-slope models only as demonstrations of structural flexibility and bases its inferential interpretation on the more stable random-intercept formulations.

For shear, the baseline model S0 produced an AIC of 1153.3 and a BIC of 1186.4. Adding subject- and task-level intercepts (S2) reduced AIC by 12.9 points and deviance by approximately 17 units, while increasing log likelihood from −563.65 (S0) to −555.18 (S2). These gains were obtained without adding fixed predictors and indicate that hierarchical structure captures real variability in shear exposure. The random-slope model S4 produced the best fit on every index, achieving the lowest AIC (1115.7), lowest BIC (1166.6), highest log likelihood (−537.87), and lowest deviance (1075.7). This improvement, however, required expanding the random structure from 42 estimated terms (S2) to 144 (S4)—more random-effect terms than the 106 observations available—raising a substantial overfitting concern that the information criteria do not fully reflect. Because the objective was to identify broadly transferable determinants of lumbar loading rather than to reconstruct individual lifting behavior, S4 was not selected despite its superior fit.

Among the reduced shear models, removing the non-significant predictors improved parsimony at almost no cost to fit, and in fact reduced BIC. AIC changed only slightly across S9 (1146.5), S10 (1145.8), and S11 (1144.3), remaining within about 4 points of S2, while BIC fell monotonically from 1178.5 (S2) to 1170.1 (S11). S11 therefore achieved the lowest AIC and the lowest BIC of the reduced shear models while carrying the simplest random structure, retaining only the subject-level intercept. It was selected as the final shear model on this basis.

For compression, the baseline model C0 produced an AIC of 1427.3. Adding subject and task intercepts (C2) reduced AIC to 1381.7 and deviance by approximately 50 units, a substantially larger absolute improvement than observed for shear and consistent with the larger residual scale of compressive loading. Adding random slopes (C4) lowered AIC further to 1370.5 and produced the highest log likelihood and lowest deviance among compression models. Unlike the shear family, however, this gain did not extend to BIC: C2 retained the lowest BIC (1419.9) compared with C4 (1421.4), indicating that the 72 additional random terms in C4 (42 → 114, again exceeding the 106 observations) were not justified once model complexity was penalized. C4 was therefore set aside on the same grounds as S4.

Compression behaved differently under reduction. Removing predictors degraded fit on both criteria: AIC rose from 1381.7 (C2) to 1397.4 (C11), and BIC from 1419.9 (C2) to 1428.3 (C11). C11 was in fact the poorest-fitting of the three reduced compression models on AIC (C8 = 1392.2; C10 = 1393.9; C11 = 1397.4). It was nonetheless selected as the final compression model because it removed knee flexion—the only non-significant predictor remaining ($p = 0.14$, C2)—yielding a model in which every retained fixed effect was significant, at a modest and acceptable cost in fit relative to C8.

Taken together, the two families behaved asymmetrically under reduction. Shear tolerated the removal of four fixed predictors and the task intercept with a negligible AIC penalty and an outright BIC improvement, indicating that much of its predictor set was redundant once load, reach, and lower-extremity posture were retained. Compression, by contrast, lost fit on both criteria with each removal, indicating that its retained posture variables carried more non-redundant explanatory information. This performance asymmetry parallels the coefficient and significance patterns of Section 3.1 and reinforces that lumbar shear and compression are not interchangeable representations of spinal loading. In both families, however, the highest-fitting specification (S4, C4) was not the most informative or deployable, and the reduced hierarchical models S11 and C11 were retained as the basis for the comparative coefficient analysis that follows.

3.3. Comparison of Fixed-Effect Coefficients Between Shear and Compression Models

Figure 1 summarizes the fixed-effect estimates across the matched shear (S) and compression (C) families and allows direct comparison of how each ergonomic and posture descriptor influences the two loading mechanisms. Although both outcomes were estimated from identical lifting data and equivalent predictor definitions, the coefficients differed substantially in magnitude and in which predictors reached significance. All values below are taken from Table A2 and all p-values from Table A3.

Load magnitude and horizontal hand position emerged as the dominant predictors of both outcomes. Both were positive, highly significant, and stable across model reduction. Load remained near 19–20 N/kg across all shear models (19.6 ± 2.3 N/kg, $p < 0.001$, S11) and near 93–105 N/kg across all compression models (105.0 ± 21.7 N/kg, $p < 0.001$, C11), a compression-to-shear sensitivity ratio of approximately five to one. Horizontal reach showed the same pattern at a smaller ratio, holding near 25–28 N/cm for shear (28.0 ± 4.1 N/cm, $p < 0.001$, S11) and near 80–100 N/cm for compression (80.8 ± 17.7 N/cm, $p < 0.001$, C11), roughly three to four times greater. The stability of both predictors across reduced formulations indicates that they act as general mechanical drivers of lumbar loading rather than outcome-specific effects, and that increasing either external load or forward reach amplifies both loading modes while affecting compression more strongly in absolute terms.

Vertical hand position produced the largest divergence between the two outcomes. Compression was consistently sensitive to vertical position (15.6 ± 2.9 N/cm, $p < 0.001$, C11), with all compression estimates significant at $p < 0.001$. The corresponding shear coefficients were roughly eight times smaller and only weakly significant (1.9 ± 0.7 N/cm, $p = 0.007$, S11), reaching borderline non-significance in the random-slope model ($p = 0.051$, S4). Both effects were positive, so vertical relocation of the load increased both outcomes, but it altered compression far more directly than shear.

Biological sex behaved similarly across the two model families in direction but not in scale. Coefficients were positive and significant throughout, remaining near 166–191 N for shear (181.8 ± 17.1 N, $p < 0.001$, S11) and near 669–855 N for compression (815.9 ± 88.3 N, $p < 0.001$, C11), a ratio of approximately four to one. Because the digital human reconstructions incorporated participant- and sex-specific anthropometric scaling, anthropometric

factors such as segment mass, body dimensions, mass distribution, and internal moment arms may contribute to this adjusted group difference. However, strength, lifting experience, and posture-selection strategies were not consistently available across the source studies and may also contribute. The sex coefficient therefore represents an adjusted difference between the male and female groups in the pooled dataset; it does not isolate a biological or behavioral mechanism, establish a causal effect of sex, or indicate sex-specific susceptibility to injury. The lower-extremity posture variables were concordant between outcomes, sharing the same sign in both families. Hip flexion was negative and highly significant throughout, near −5 to −6 N/deg for shear (−5.6 ± 0.7 N/deg, $p < 0.001$, S11) and roughly two to three times larger for compression (−12.6 ± 2.7 N/deg, $p < 0.001$, C11); greater hip flexion reduced both loading modes. Knee flexion was positive in both families and of similar magnitude (3.9 ± 0.6 N/deg for shear; 3.3 ± 2.3 N/deg, C10, for compression), but it diverged on significance: significant for shear at every stage ($p < 0.001$, S11) yet never significant for compression in any hierarchical model ($p = 0.14$, C2), which is why it was retained only in the shear models. Elbow flexion was negative and significant in both final models, near −1.8 N/deg for shear ($p < 0.001$, S11) and approximately four times larger for compression (−7.1 ± 1.9 N/deg, $p < 0.001$, C11), though it reached significance for compression only once random intercepts were added ($p = 0.39$, C0; $p = 0.004$, C2).

Trunk and shoulder flexion separated the two outcomes most clearly. Trunk flexion was a substantial, significant negative predictor for compression (−10.3 ± 3.3 N/deg, $p = 0.002$, C11) but negligible and non-significant for shear at every stage (−0.87 ± 0.84 N/deg, $p = 0.31$, S2), which is why it was dropped from the shear models. Shoulder flexion showed the same selectivity: significant and positive for compression in the hierarchical models (6.7 ± 2.0 N/deg, $p = 0.001$, C11) but small and non-significant for shear (0.67 ± 0.67 N/deg, $p = 0.31$, S2). Both variables changed sign between the fixed-only and hierarchical specifications (shoulder flexion from −3.7 to +4.8 N/deg, C0 to C2), reinforcing that the fixed-only estimates should be read with caution.

Two predictors did not show stable independent associations with either loading outcome. Shoulder abduction/adduction was non-significant throughout both families (0.32 ± 0.61 N/deg, $p = 0.60$, S2; −1.46 ± 1.98 N/deg, $p = 0.46$, C2) and was removed from both. Coupling quality was likewise non-significant, with a wide confidence interval in compression (−79.5 ± 204.4 N, $p = 0.70$, C2) and a comparatively small estimate in shear (−9.8 ± 29.4 N, $p = 0.74$, S2). It was therefore removed during the outcome-specific model-reduction pathways. These results indicate that neither variable explained additional variation in peak L4/L5 compression or anterior–posterior shear after load geometry and gross posture were included. The complete outcome-specific reduction analyses are reported in [26,27].

Taken together, the coefficient comparison shows that compression and shear share common deterministic drivers but respond differently to posture. Load magnitude and horizontal reach dominated both outcomes with the same sign, differing only in scale. The clearest distinctions appeared for vertical position, trunk flexion, and shoulder flexion, all of which influenced compression substantially more than shear, and for knee flexion, which was significant only for shear. Critically, no predictor that was significant in both families reversed sign between them: every shared effect acted in the same direction, and the divergence between outcomes lay in magnitude and in which predictors reached significance rather than in the direction of their influence. This pattern indicates that equivalent changes in lifting posture do not propagate uniformly across the two loading components, even though both are driven by the same external task variables.

A final consideration concerns the uncertainty associated with these estimates. The compression coefficients carried larger absolute confidence intervals than their shear coun-

terparts for nearly every predictor, most visibly for load, horizontal and vertical position, and the posture angles. This difference is largely attributable to the scale of the loading outcome rather than to reduced model stability. In the pooled dataset, mean L4/L5 compression force (2762 N) was approximately 4.8 times mean anterior–posterior shear force (580 N), and the corresponding standard deviation (1264 N versus 315 N) and range (6195 N versus 1557 N) were approximately four times larger (Table 1). The compression confidence intervals scale with this larger mechanical range, so that the dominant predictors retained stable point estimates across successive formulations despite their wider absolute bands. The precise normalization of residual error to mean force, which confirms comparable relative precision between the two families, is presented in Section 3.4.

3.4. Comparison of Random Effects and Variance Structure

To identify the sources of variability underlying spinal loading, the random-effect structures of the two model families were compared (Table 4). Whereas the fixed effects describe average relationships across all observations, the random effects describe how those relationships vary across subjects and tasks, and therefore characterize the reproducibility and subject dependence of each loading mechanism.

Table 4. Random Factor Regression Coefficients and residuals for the Anterior–Posterior Shear force model (Si) and Compression force model (Ci). "—" indicates that the corresponding random-effect component was not included in the model and therefore no standard deviation was estimated.

	StudyID_SD	SubjectID_SD	TaskID_SD	Load_slope_SD	H_slope_SD	Residual_SD
S0	—	—	—	—	—	60.13
S2	—	43.641	16.336	—	—	44.19
S4	—	316.71	15.866	5.702	6.859	24.49
S9	—	42.733	10.618	—	—	44.196
S10	—	39.836	10.866	—	—	44.96
S11	—	39.606	—	—	—	45.488
C0	—	—	—	—	—	258.23
C2	—	233.78	140.15	—	—	135.88
C4	—	710.81	131.69	21.24	15.43	90.71
C8	—	233.51	107.84	—	—	135.78
C10	—	234.01	106.5	—	—	135.2
C11	—	240.17	108.91	—	—	134.68

For both outcomes, introducing hierarchical structure substantially reduced unexplained variance. In the fixed-only models, all unexplained variability was absorbed into the residual term, yielding residual standard deviations of 60.13 N (S0) and 258.23 N (C0). Adding subject- and task-level intercepts reduced these values sharply, indicating that a meaningful share of spinal loading variability arises from systematic differences between individuals and conditions rather than from measurement noise.

The reduction was pronounced for shear. Residual variability fell from 60.13 N (S0) to 44.19 N (S2), and reached its minimum of 24.49 N (S4) once random slopes for load and reach were added, an overall reduction of approximately 59% relative to the fixed-only baseline. Compression followed the same pattern at a larger absolute scale: residual SD fell from 258.23 N (C0) to 135.88 N (C2) and further to 90.71 N (C4), a reduction of approximately 65%. In proportional terms the residual gain from adding slopes was actually larger for shear (a 45% drop from S2 to S4) than for compression (33% from C2 to C4).

The larger absolute residuals of the compression models reflect the scale of compressive loading rather than poorer fit. Mean L4/L5 compression force (2762 N) was approximately 4.8 times mean shear force (580 N), and the baseline residual SD was approx-

imately 4.3 times larger (258 N versus 60 N). Normalized to mean force, the two baseline residuals are nearly identical, representing approximately 9.3% of mean compression force (C0) and 10.4% of mean shear force (S0). This is the residual-normalization comparison referenced in Section 3.3, and it holds across the hierarchy: relative residuals remained in the single-digit-percentage range for both families at every formulation, confirming comparable relative predictive precision despite the different force scales.

Across all hierarchical formulations, subject-level variability was the dominant random component. In the shear family, the SubjectID intercept SD remained near 40–44 N in the random-intercept models (43.6 N, S2; 39.6 N, S11), while the TaskID SD stayed comparatively modest at approximately 11–16 N (16.3 N, S2; 10.6 N, S9). Relative to mean shear force, these correspond to roughly 7–8% subject variability and only 2–3% task variability. Compression showed the same ordering at larger magnitude: the SubjectID SD exceeded 230 N in every random-intercept model (233.8 N, C2; 240.2 N, C11) while the TaskID SD ranged from approximately 106 to 140 N (140.2 N, C2; 108.9 N, C11), corresponding to roughly 8% subject and 4–5% task variability. In both families, then, differences in how individuals performed the same lift contributed more variability than differences between lifting conditions.

The difference in the magnitude of the task-level component explains the asymmetric final random-effects structures. For shear, removing TaskID between S10 and S11 eliminated a comparatively small variance component while slightly improving AIC and BIC and leaving the principal fixed-effect estimates essentially unchanged. For compression, the task-level component remained non-negligible through C11 and was therefore retained. The final structures should thus be interpreted as outcome-specific results of variance partitioning rather than as an assumption that tasks influence only compression.

The random-slope models require more careful interpretation. The estimated slope SDs in S4 were 5.70 N/kg for load and 6.86 N/cm for horizontal reach, indicating moderate subject-to-subject variability in sensitivity to external demand; the corresponding values in C4 were larger in absolute terms at 21.24 N/kg and 15.43 N/cm. Expressed relative to their fixed-effect coefficients, however, this variability was proportionally greater for shear: subject variability in the horizontal-reach slope was approximately 27% of the fixed reach effect for shear (6.86 N/cm against 25.6 N/cm, S4) versus approximately 15% for compression (15.43 N/cm against 99.85 N/cm, C4), with load showing the same direction (roughly 29% versus 21%). This suggests that individuals differ more in how forward reach translates into shear than into compression.

The accompanying jump in the SubjectID intercept SD at this stage—from 43.6 N (S2) to 316.7 N (S4), and from 233.8 N (C2) to 710.8 N (C4)—should not be read as a genuine increase in baseline between-subject variability. Once random slopes are introduced, the intercept term represents subject deviation at load = 0 kg and reach = 0 cm, an extrapolated condition well outside the observed range (load $\geq$ 5 kg, H $\geq$ 35 cm), and the intercept–slope covariance inflates it. The interpretable subject-level quantities in S4 and C4 are therefore the slope SDs rather than the intercept SD, and the instability of this intercept term is consistent with the overparameterization that led both random-slope models to be set aside (Section 3.2).

Model reduction had little effect on the random-effect estimates. SubjectID variability in the shear family remained between approximately 40 and 44 N across S2, S9, S10, and S11, and the compression estimates stayed clustered near 234–240 N across C2, C8, C10, and C11; residual SDs likewise changed by less than 2 N across each family's reduced models. This stability indicates that the hierarchical structure of the data is robust and that subject-dependent variability persists even after substantial simplification of the fixed-effect architecture.

Overall, both lumbar shear and compression were strongly shaped by subject-specific behavior, with subject-level variability exceeding task-level variability throughout. Compression exhibited greater absolute heterogeneity, but once normalized to the underlying force scale, the random-intercept and residual structures of the two families were comparable. The dominance of subject effects over task effects, together with the modest task-level variability that remained after the fixed predictors were accounted for, indicates that individual lifting strategy is a central determinant of spinal mechanical exposure and supports the use of hierarchical modeling for both outcomes.

3.5. Cross-Classification of Compression and Shear Reference Values

To quantify the extent to which a compression-only classification may overlook elevated shear loading, the 106 complete-case observations were cross-classified using 3.4 kN as the compression criterion and 700 N as the lower shear reference cited in the literature. Ninety-one observations (85.8%) remained below both values, 11 observations (10.4%) remained below the compression criterion while exceeding 700 N shear, no observations exceeded the compression criterion while remaining below the shear reference, and four observations (3.8%) exceeded both values. Thus, among the 102 observations classified below the compression criterion, 11 (10.8%) nevertheless exceeded the 700 N shear reference. No observation below 3.4 kN compression exceeded the upper 1000 N shear reference, indicating that the degree of discordance depends on the selected shear reference.

4. Discussion

4.1. Shared Determinants and Divergent Sensitivities of Lumbar Loading

The aim of this study was not to establish whether compression or anterior–posterior shear is the more important indicator of injury risk, but to examine how identical ergonomic and postural variables influence the two loading pathways when estimated within a common biomechanical and statistical framework. Because both model families were derived from the same lifting tasks, the same digital human simulations, equivalent predictor definitions, and parallel mixed-effects architectures, the differences between them can be attributed to how spinal loading is mechanically distributed rather than to differences in experimental design or data processing. Within this controlled comparison, the principal finding is that some ergonomic variables act as universal determinants of spinal loading while others selectively shape the demand carried by one pathway more than the other.

Two variables behaved as universal drivers. Load magnitude and horizontal hand position were positive, highly significant, and stable across every model formulation and through model reduction (Sections 3.1 and 3.3). Their persistence in both families confirms that they represent general mechanical determinants of lumbar loading rather than outcome-specific predictors [40], and it reinforces the biomechanical premises of the Revised NIOSH Lifting Equation, which identifies object weight and forward reach as the primary contributors to lifting difficulty. The two outcomes differed in the scale of their response—compression was several times more sensitive to both variables in absolute terms—but they agreed in sign and in significance throughout, so the practical implication is shared: reducing load and minimizing horizontal reach lower both compression and shear.

The posture variables told a different and more informative story. Rather than influencing the two outcomes uniformly, they separated them. The shear models retained knee flexion while discarding trunk and shoulder flexion; the compression models retained trunk and shoulder flexion while discarding knee flexion (Section 3.1). Vertical hand position, trunk flexion, and shoulder flexion exerted a substantially stronger influence on compression than on shear, whereas knee flexion was significant only for shear (Section 3.3). This near mirror-image divergence in which posture descriptors matter—together with the asym-

metric fit behavior under reduction (Section 3.2) and the differing random-effects structure (Section 3.4)—indicates that compression and shear are governed by partly distinct postural determinants even when the external task is held identical.

Coupling quality requires a narrower interpretation. Its persistent non-significance across the compression and shear model families does not establish that coupling is irrelevant to lifting safety. Poor coupling may affect grasp security, slip risk, object controllability, perceived exertion, and the need for compensatory stabilization even when it does not produce a measurable independent change in peak lumbar force. The present result indicates only that the binary good-versus-poor coupling indicator did not explain additional variation in modeled L4/L5 compression or anterior–posterior shear after load magnitude, hand location, and whole-body posture were controlled. The wide compression confidence interval may also reflect the limited resolution of the harmonized binary coding, which cannot distinguish more detailed differences in handles, friction, object shape, or grip strategy. The published outcome-specific analyses provide the complete model-reduction results for this variable [26,27].

A second feature of this divergence is as important as the divergence itself: among the predictors that were significant in both families, none reversed sign. Every shared effect acted in the same direction in both outcomes, and the differences between compression and shear lay entirely in magnitude and in which predictors reached significance, not in the direction of their influence (Section 3.3). The two loading components are therefore neither interchangeable nor opposed. They are related but non-equivalent responses to the same external demand, which means that evaluating a single loading metric—as conventional compression-anchored assessment does—can miss how a given lifting strategy distributes mechanical demand within the lumbar spine. The remainder of this discussion develops the implications of this result: that posture acts as a selective modulator rather than a redistributor of spinal load (Section 4.2), that this selectivity follows from compression and shear tracking two distinct geometric quantities—the moment arm of the supported mass and the orientation of the lumbar segment (Section 4.3), that the resulting subject-specific variability is a structural rather than incidental feature of lumbar loading (Section 4.4), and that together these point toward a multidimensional reframing of ergonomic assessment (Section 4.5).

4.2. Posture as Selective Modulation Rather than Redistribution

If load magnitude and horizontal reach set the magnitude of the mechanical challenge, the posture variables determine how that challenge is accommodated. The central question this section addresses is the form of that accommodation: whether posture redistributes demand between the two loading pathways—relieving one by loading the other—or whether it modulates them independently. These are distinct mechanical claims with distinct empirical signatures, and the present data discriminate between them.

The two hypotheses make opposite predictions about coefficient signs. If posture acted as a redistribution mechanism, re-dividing a single spinal reaction between its two components, then a postural change that relieves one loading component should load the other, and the two outcomes would show antagonistic coefficients—opposite signs for the same predictor. A trade-off between compression and shear would appear as a variable that is negative in one family and positive in the other. If instead posture modulates the two pathways independently, shared predictors would retain the same sign in both outcomes and differ only in how strongly each pathway responds. Redistribution predicts sign reversal; selective modulation predicts sign agreement with divergent magnitude.

The results fall unambiguously on the modulation side. Among the predictors significant in both families, not one reversed sign (Section 3.3). Every shared effect acted in the

same direction for compression and shear, and the differences between the two outcomes lay in magnitude and in which predictors reached significance, never in direction. Posture did not trade compression for shear; it set the degree to which each pathway responded to the fixed external demand.

The coefficient structure can be organized into three classes, and the distance- and orientation-based geometry developed in Section 4.3 explains why each class exists. The first comprises concordant variables, which carried the same sign in both outcomes because they act on a quantity that feeds both reaction components. Hip flexion is the clearest example: by setting the orientation of the column it influences shear, and by governing how the trunk and its mass are carried forward it influences the compressive moment arm, so it appeared in both families with the same negative sign and comparable consistency. Elbow flexion behaves likewise, drawing the load toward the body and shortening the moment arm while producing a small accompanying change in segment orientation, so that it too remained negative and significant in both outcomes. Variables of this class function as shared drivers of spinal loading rather than as redistributors.

The second class comprises outcome-selective variables, which kept a consistent sign across outcomes but acted far more strongly on one component because they change predominantly one of the two governing geometric quantities. Trunk flexion and shoulder flexion belong here on the compression side: trunk-on-pelvis flexion throws the upper-body mass ahead of L4/L5 and shoulder flexion reaches the load outward, both lengthening the moment arm without reorienting the lumbar segment, and both accordingly remained important throughout the compression reduction while becoming negligible for shear. Vertical hand position showed the same compression-weighted selectivity. Knee flexion is the corresponding shear-selective variable, altering pelvic tilt and column orientation while leaving the moment arm comparatively unchanged, and it was retained for shear while pruned from compression. Variables of this class do not act on both pathways equally; they preferentially load the component whose governing geometry they control.

The third class—antagonistic variables, carrying opposing signs across outcomes—would be the signature of genuine redistribution, in which a postural change relieves one component by loading the other. This class was empty: no predictor occupied it. Its absence is informative because antagonism is not a strawman but the specific prediction of an intuitive and competing mechanical model. If compression and shear were two projections of a single conserved reaction vector onto the segment's axes, then a postural change that rotated those axes would re-divide the fixed resultant between them, growing one component while shrinking the other—an opposite-sign, trade-off relationship. The empty antagonistic class falsifies that shared-resultant picture. Compression and shear do not behave as rival slices of one conserved quantity, because they are not sourced from one: compression is driven by the moment arm of the supported mass, which sets the magnitude of the balancing demand, while shear is driven by the orientation of the lumbar segment, which sets the in-plane share of the vertical load. The moment arm is not conserved across postures—it lengthens and shortens with configuration—so there is no fixed budget to redistribute, and a change that increases one component need not deplete the other. The sign pattern in the data therefore discriminates between two candidate mechanisms and selects the second: posture does not re-slice a single reaction but independently modulates two separately sourced quantities. This is precisely the account developed mechanistically in Section 4.3.

This reframing also clarifies an apparent puzzle in the posture coefficients that a purely external lever-arm interpretation of lifting would get wrong. Several variables that intuitively increase the external moment carried a negative coefficient. Trunk flexion, for example, was strongly negative for compression despite the familiar observation that

leaning forward while holding a load generally increases lumbar demand. The resolution is that the regression coefficients are conditional effects: they describe how loading differs with joint configuration while horizontal and vertical hand position are held fixed, rather than the total effect of a movement that also changes the location of the load. Because hand position is already included in the model, the direct mechanical consequence of moving the load farther from the body has been accounted for. The posture coefficients instead compare alternative whole-body configurations used to reach the same hand position.

A numerical example illustrates the distinction. In the matched random-intercept models, the trunk-flexion coefficient was approximately −10.98 N/degree for compression (C2) and −0.87 N/degree for anterior–posterior shear (S2). Holding load magnitude, hand position, and all other predictors constant, a 10° increase in trunk flexion therefore corresponds to an approximately 110 N reduction in predicted compression but only an approximately 9 N reduction in predicted shear; the shear coefficient was not statistically significant. The final compression model produced a similar estimate of approximately −10.28 N/degree, equivalent to about 103 N for a 10° difference. These values compare configurations that achieve the same external hand location. They do not imply that bending forward while simultaneously moving the load farther from the body reduces lumbar compression.

The coefficients therefore describe alternative postures that achieve identical task geometry, not the uncontrolled effect of moving a single rigid segment. The geometric basis for why these conditional effects separate compression from shear is developed in Section 4.3.

Finally, the divergent reduction pathways reinforce the modulation interpretation at the level of model structure. The shear models converged toward a compact set dominated by load, reach, and lower-extremity posture, whereas the compression models retained sensitivity to a broader range of body configurations including trunk and shoulder posture (Sections 3.1 and 3.2). This asymmetry is consistent with the two geometric channels: shear is shaped largely by the orientation the lower body imposes on the lumbar segment, while compression remains sensitive to every configuration that changes how far the supported mass acts from the spine. Posture, in this view, is not a switch that routes load between two channels but a regulator that sets how strongly each channel responds to the fixed external demand—most consequentially for compression, the pathway governed by the moment arm and therefore sensitive to the widest range of postural choices.

4.3. A Mechanistic Account: Distance, Orientation, and the Geometry of the L4/L5 Reaction

The empirical patterns of Sections 4.1 and 4.2 follow from how the lumbar reaction is generated in the underlying biomechanical model, and that generation is governed by geometry rather than by muscle. In the digital human model used to produce the loading estimates, the body is treated as an open kinematic chain described by the joint-angle vector $\mathbf{q}$, with both ends effectively constrained: the feet against the ground and the hands against the load. The external load, which under gravity acts vertically, is mapped to the generalized joint loads through the transpose of the chain's Jacobian, $\boldsymbol{\tau} = \mathbf{J}^{\mathrm{T}}(\mathbf{q})\,\mathbf{F}$, where $\mathbf{J}^{\mathrm{T}}(\mathbf{q})$ carries the moment arms relating the hand force to the loads borne at each joint [36,38]. The intersegmental reaction at L4/L5 is then recovered from a free-body diagram of the segments above the cut, and its two reported components are expressed in the segment's own moving frame: compression acts along the endplate normal, into the disc, and anterior–posterior shear acts within the endplate plane. No muscle forces, recruitment rules, or tissue properties enter this calculation, so the differences between the two loading components are differences in geometry alone.

This framing makes load magnitude and horizontal reach the universal drivers they appear to be in the data. Together they set how heavy the supported system is and how far it acts from the lumbar spine, and therefore they fix the overall size of the reaction the spine must supply. This is the part of the problem that any simple lever model captures, and it is why these two variables dominate both outcomes and persist through model reduction (Section 3.3). Posture enters only afterward, by determining how that fixed demand is shared between the two reaction components.

The key to the divergence between compression and shear is that the two components respond to two distinct geometric quantities. Compression is governed chiefly by the demand to balance the moment that the supported mass exerts about L4/L5, and that moment scales with the horizontal distance between the lumbar segment and the line of action of the load and upper-body mass. Compression therefore tracks a distance—the moment arm. Anterior–posterior shear, by contrast, is governed by the orientation of the L4/L5 segment relative to the vertical load: the more the segment is tilted away from upright, the larger the share of the vertical demand that falls within the endplate plane [41]. Shear therefore tracks an angle—the segment tilt. Because a distance and an angle are independent geometric properties, a postural change can alter one substantially while leaving the other nearly unchanged, which is precisely the selective behavior observed in Section 4.2 and which a single rigid lever, with its one rigidly linked reaction, cannot reproduce.

The reason a longer moment arm registers specifically as compression follows from a two-step balance of moments about the disc. The external load, acting at a horizontal distance from the lumbar joint, imposes a flexing torque equal to its magnitude times that distance; lengthening the moment arm—by moving the load forward or flexing the trunk over it—increases this torque proportionally. Equilibrium requires the segment to generate an equal and opposite restoring torque, and this is supplied by the posterior extensor structures, which act at a short moment arm behind the disc center—on the order of 5–6 cm [42]—that is fixed by anatomy and does not change with posture. Because that internal moment arm is small and essentially constant, the restoring force needed to balance the external torque is large—the external load scaled up by the ratio of the long external arm to the short fixed internal arm—and because it acts nearly along the axis of the spine, it is transmitted to the disc almost entirely as axial compression. A longer external moment arm therefore cannot be accommodated by recruiting a longer lever; it can only be met by a larger axial force, so the compressive reaction rises in proportion to the moment arm. The scale of this amplification is substantial: the horizontal hand distances in the present dataset ranged from 35 to 95 cm (Table 1), roughly an order of magnitude greater than the fixed posterior arm, so modest changes in load position produce large changes in compression—consistent with the compression sensitivities exceeding their shear counterparts severalfold (Section 3.3). It should be noted that the digital human model does not compute muscle forces explicitly; the intersegmental compression it reports is the static equivalent of this balance, in which the moment imposed by the external load is resisted by a force acting at the fixed posterior offset. Whether expressed as an extensor force or as the moment-resisting reaction at the joint, the resulting axial load on the disc is the same.

This distance-versus-orientation distinction sorts the posture variables almost exactly as the model reduction did. Trunk flexion, measured relative to the pelvis, is the flexion across the lumbar cut itself; flexing the trunk forward on the pelvis throws the upper-body mass ahead of L4/L5 and lengthens its moment arm, so it acts strongly on compression and was retained throughout the compression reduction while contributing little to shear (Sections 3.1 and 3.3). Shoulder flexion reaches the load outward from the trunk, lengthening the moment arm of the load without reorienting the lumbar segment, and so it too

attached to compression alone. Hip and knee flexion behave oppositely: they set pelvic tilt and lower-limb geometry and therefore the orientation of the whole column, so they act on shear, with knee flexion retained in the shear family and absent from compression. The pruning pattern is thus not an artifact of model selection but the expected footprint of a distance channel and an orientation channel acting on different parts of the same chain.

Two variables sit in both families, and the geometry explains why. Hip flexion changes the orientation of the column, which feeds shear, but it also governs how the trunk and its mass are carried forward, which feeds the compressive moment arm; it therefore appears in both outcomes with the same negative sign, and it is the clearest example of a shared driver rather than a redistributor. Elbow flexion is similar but weighted toward compression: because the recorded postures are predominantly flexed at the elbow, increasing elbow flexion draws the forearm and load toward the body, shortening the moment arm and reducing compression directly, while producing only a small accompanying change in segment orientation. This accounts for elbow flexion being significant in both families with the same sign yet several times larger for compression than for shear (Section 3.3); its shear contribution is best read as a modest geometric by-product of a primarily distance-changing joint rather than as evidence that the elbow is an orientation driver.

The same distinction explains why shoulder and elbow, though both arm joints distal to the cut, behave so differently with respect to shear. A useful test for any joint is whether moving it changes the orientation of the L4/L5 segment or only the distance of the supported mass from it: orientation changes feed shear, distance changes feed compression, and joints that do both—the trunk-on-pelvis flexion and the hip—feed both. Shoulder flexion changes distance only, because reaching the arm forward relocates the load relative to the spine without tilting the lumbar segment, and so it is compression-specific. Elbow flexion changes distance and, at a fixed hand position, a small amount of orientation, and so it is shared but compression-weighted. The criterion sorts every predictor, including the one that simpler accounts mishandled.

It is this conditioning on hand position that resolves the apparent sign paradox introduced in Section 4.2. Because horizontal and vertical hand location are already included as predictors, each posture coefficient describes the effect of reconfiguring the chain to reach the same hand position by a different route, not the total effect of a raw joint motion that also moves the load. The negative compression coefficient for trunk flexion therefore does not contradict the everyday fact that bending forward over a load is taxing; it reports that, among the configurations that place the hands at one fixed location, those involving greater trunk flexion correspond to a redistribution of the supported mass that shortens its effective moment arm and lowers compression. Each coefficient is a partial sensitivity of the equilibrium reaction to internal reconfiguration at fixed endpoints, and the raw lever-arm intuition misleads only because it conflates this conditional effect with the total one.

Two points of restraint frame these results. The mechanics invoked here—the balance of an external moment, the transmission of force across an inclined segment, and the redundancy of an open multi-link chain—are established principles of occupational biomechanics, and the present analysis does not claim to have discovered them. What the analysis contributes is the demonstration that these distinctions are recoverable from accessible task and posture descriptors, and that compression and shear separate empirically along exactly the distance- and orientation-based lines the geometry predicts. Equally, the reported coefficients are linearized, population-level sensitivities estimated over a broad but finite range of postures; they summarize the average direction and scale of these conditional effects rather than the full nonlinear dependence of the reaction on configuration.

A final observation concerns where this determinism ends. The map from configuration $\mathbf{q}$ to the L4/L5 free-body diagram is rigid: once posture is specified, the reaction and

its two components follow from statics alone. What is not fixed is the configuration itself. Faced with a constant external demand, each lifter had to select a posture from the many that reach the load, and that selection is a behavioral act rather than a mechanical one. Had those selections been arbitrary or uniformly spread across the joints, the regressions would not have resolved into two compact, distinctly pruned models; that they did indicates that postural choice is itself organized, with lifters systematically adjusting the orientation of the lower body in ways that bear on shear while separately organizing the distance of the supported mass in ways that bear on compression. The mechanics are deterministic, but the coordination that supplies their inputs is not—an observation that motivates the analysis of subject-specific variability in Section 4.4.

4.4. Subject-Specific Variability as a Structural Feature of Lumbar Loading

The mechanistic account of Section 4.3 ends at a deliberate boundary: the map from posture to spinal reaction is fixed by statics, but the posture itself is chosen. This section takes up that chosen part. Faced with a load they could not change, lifters had to select one configuration from the many that reach it, and the random-effects structure of the models provides a direct window onto how that selection was organized. Read biomechanically, the variance components describe not statistical nuisance but the consequences of individual lifting strategy.

The clearest result concerns the relative ordering of the variance components rather than their absolute size: subject-level variability exceeded task-level variability for both outcomes and at every stage of model reduction (Section 3.4). In the shear models the between-subject intercept standard deviation remained near 40 N, approximately 6.9% of the 580 N mean shear force, while the between-task standard deviation stayed near 11–16 N, roughly 1.9–2.8% of that mean. In the compression models the between-subject term remained near 234–240 N, approximately 8.5–8.7% of the 2762 N mean compression force, against a between-task term near 107–140 N, roughly 3.9–5.1% of that mean. Normalized to the mean force of each outcome, between-subject variability was therefore roughly twice the between-task variability in both families. The lifting condition—the load, its location, the nominal task—accounted for less of the remaining spread in spinal loading than did the identity of the person performing it. Two workers presented with the same lift arrived at systematically different lumbar loads, and they did so consistently enough that subject identity remained a stable variance component after the fixed predictors had absorbed the average effects of load, reach, and posture.

The residual task-level component nevertheless differed between the two loading outcomes. Its comparatively small magnitude and removal from S11 suggest that the measured hand coordinates and posture variables captured most systematic task-to-task differences relevant to lumbar orientation and anterior–posterior shear. The persistence of TaskID in C11 suggests that task identity carried additional information relevant to compression that was not represented fully by the measured predictors. One possible explanation is that compression integrates the moment effects of both the external load and the distributed masses of the upper body and may therefore remain sensitive to unmeasured task characteristics such as object geometry, hand separation, mass distribution, external support, contact constraints, or other details of task execution. This interpretation remains provisional. Because TaskID aggregates several task characteristics, the present models cannot determine which specific feature generated the remaining compression variance. Explaining why task-level variability persists for compression but not for shear therefore remains an open research question.

The persistence of this term is more telling than its magnitude, and it bears directly on a natural objection. A nonzero subject variance can, in principle, indicate model

inadequacy—unmodeled fixed-effect structure leaking into the random term—rather than genuine between-person differences. Two features of the present results argue against that reading. First, the subject-level standard deviation was essentially invariant under model reduction, changing by only a few percent across six successive specifications (approximately 40 N, or 6.8–6.9% of mean shear, across S2 through S11, and 234–240 N, or 8.5–8.7% of mean compression, across C2 through C11) even as predictors were added and removed; a term that merely absorbed missing fixed structure would be expected to shift as that structure was respecified. Second, the subject variance did not compete with the fixed effects for explanatory share but coexisted with a stable residual term, indicating that it captures dependency among repeated observations of the same individual rather than systematic effects the fixed part failed to model. The subject component therefore behaves as a genuine grouping effect, not as a symptom of a weak regression.

A second and more substantive source must be considered before attributing this variability to lifting behavior: subjects differ in body size, and larger individuals generate larger L4/L5 forces performing an identically defined task simply because their own segment masses are greater and their internal moment arms longer. Because the digital human reconstructions were scaled to each participant's anthropometry, the subject intercept reflects genuine per-subject body geometry rather than a modeling artifact, and anthropometric variation is therefore expected to contribute to it. The magnitude of that contribution can be bounded, however, by comparison against the sex term, which was modeled as a fixed effect and which captures the largest and most systematic axis of anthropometric difference [43]. The sex coefficient accounted for roughly 30% of mean force in both families (815.9 N, or 29.5% of mean compression; 181.8 N, or 31.3% of mean shear), whereas the residual between-subject standard deviation was only 6.9% of mean shear and 8.5–8.7% of mean compression—between three and four-and-a-half times smaller than the sex effect in each outcome. Because the digital human reconstructions were scaled to each participant's anthropometry, body geometry is expected to contribute to both the fixed sex coefficient and the subject-level random effect. However, the relative anthropometric and behavioral contributions cannot be quantified or bounded by comparing the magnitudes of these two terms. The fixed sex term accounts for the estimated average difference between the male and female groups after adjustment for the measured task and posture variables. It does not, however, isolate a uniquely anthropometric or biological mechanism, nor does it remove all body-size variation from the subject random effect. Variation in stature, body mass, segment proportions, strength, lifting experience, and posture-selection strategy remains within each sex group and may contribute to the residual subject-level variance. The subject intercept is therefore best understood as a mixture of unmeasured anthropometric and task-execution differences that the present dataset cannot partition further. The principal conclusion of this section, however, does not rest on resolving that mixture. Body size scales a person's loading but does not predict that the posture variables should separate into a distance channel and an orientation channel, nor that knee flexion should attach to shear while trunk and shoulder flexion attach to compression. That structure resides in the fixed effects and the pruning pattern, and is explained by the geometry of Section 4.3 rather than by how large the lifter is. The organized, mechanism-aligned character of the posture effects therefore stands independent of how the subject variance ultimately partitions between anthropometry and behavior.

This ordering is consistent with the redundancy of the kinematic chain, of which individual posture selection is one component alongside the anthropometric differences just discussed. Because many configurations satisfy the same external task, the external task cannot by itself determine the internal load; the remaining degrees of freedom are resolved by the lifter, and different lifters resolve them differently and characteristically.

The subject random effect is the statistical signature of that residual freedom together with subject body geometry—the trace of the choice the mechanics leave open, and precisely the quantity that a single-posture or task-only description of lifting necessarily omits. Its stability across the reduced models indicates that this dependency is a structural property of the data rather than an artifact of any one specification.

The random-slope models sharpen this picture but require careful reading. Allowing subject-specific sensitivities to load and reach produced the best raw fit, yet the accompanying expansion of the random structure to more parameters than observations, and the inflation of the subject-intercept standard deviation to 316.7 N for shear (54.6% of mean shear force) and 710.8 N for compression (25.7% of mean compression force), marks those formulations as overparameterized rather than newly informative (Sections 3.2 and 3.4). The inflated intercepts do not describe a real increase in baseline between-subject differences; they are an extrapolation artifact, since once slopes are present the intercept measures subject deviation at zero load and zero reach, a condition far outside the observed range. The interpretable subject-level quantities in these models are therefore the slope standard deviations. These indicate that individuals differed in how strongly forward reach translated into spinal load, and that the dispersion of those individual sensitivities, expressed as a fraction of the corresponding mean effect, was greater for shear than for compression—the between-subject standard deviation of the horizontal-reach slope was about 27% of the fixed reach effect for shear (6.86 against 25.0 N/cm) but about 15% for compression (15.43 against 99.85 N/cm). This is consistent with the mechanistic division of Section 4.3: the moment-arm geometry that drives compression is more tightly constrained by the task, whereas the segment-orientation geometry that drives shear, governed by the lower body, admits more individual variation, anthropometric and behavioral. The comparison is offered as consistent with the geometric account rather than as independent confirmation of it, since the slope variance components are estimated less precisely than the intercepts.

The organization of this variability is as important as its ordering. Had lifters resolved the redundant degrees of freedom arbitrarily, the regressions would not have separated into two compact, distinctly pruned models; the posture predictors would have entered both outcomes diffusely and inconsistently. Instead the predictors sorted cleanly along the distance-versus-orientation lines developed earlier, which means the individual differences were not undifferentiated scatter across all joints but structured choices concentrated in the degrees of freedom that matter for each loading component. Lifters varied in how they oriented the lower body, with consequences for shear, and separately in how they positioned the supported mass, with consequences for compression, rather than varying uniformly across the chain. Subject-specific variability is thus not diffuse residual error but a structured, reduction-resistant component: consistently ordered above task-level variability, stable across specifications, and concentrated in the degrees of freedom the geometry identifies as load-relevant.

These observations carry a practical implication that Section 4.5 develops more fully. Because person-level differences were consistently ordered above task-level differences, an assessment framework that characterizes a lift solely by its external parameters—load, height, reach—captures only part of the variability in actual spinal exposure and omits the posture-dependent share that depends on who is lifting and how. The ordering of the variance components is a quantitative argument that how a load is lifted is consequential alongside what is lifted, and that ergonomic evaluation aimed at the internal loading environment will benefit from observing posture, not task parameters alone.

4.5. Implications for Ergonomic Assessment

The findings of this study bear on a long-standing convention in occupational ergonomics: the interpretation of lumbar loading primarily, and often exclusively, through axial compression. The Revised NIOSH Lifting Equation and the screening practices built around it are historically anchored to compressive thresholds at the lumbosacral joint, and this anchoring has shaped both industrial practice and a large share of ergonomic research toward treating compression as the dominant indicator of lifting risk. The paired analysis presented here gives a quantitative reason to regard that single-metric framing as structurally incomplete rather than merely partial.

The central result supporting this is that compression and shear, estimated from identical lifting data under matched model structures, proved to have partly distinct determinants. They shared their dominant external drivers—load magnitude and horizontal reach—but diverged in their posture sensitivities along interpretable geometric lines: compression governed by the distance at which the supported mass acts from the lumbar spine, shear by the orientation of the lumbar segment. Because the two components respond to different geometric quantities, a lifting configuration that is favorable for one is not guaranteed to be favorable for the other, and a metric that tracks only compression cannot by construction report the shear consequences of a given posture. This matters precisely because, as the literature this study builds on has argued, shear loading is associated with injury mechanisms—disc herniation, vertebral slippage, facet degeneration—at magnitudes that can fall below established compressive safety thresholds. An assessment that is blind to shear is therefore blind to a pathway of tissue stress that compression does not predict.

The practical consequence is that reducing the two loading components can call for different interventions. Lowering compression is, in geometric terms, a matter of shortening the moment arm of the supported mass—drawing the load toward the body and limiting forward trunk inclination over it. Lowering shear is more a matter of segment orientation, governed by how the lower body sets the tilt of the lumbar column. These are not the same instruction, and they are not jointly optimized by a single compression-based guideline. A framework that recognizes both components can, in principle, distinguish a posture that protects the disc from axial load but leaves it exposed to shear from one that manages both, a distinction that a one-dimensional metric cannot express.

A further implication follows from the variance structure rather than the coefficients. Because between-subject variability was consistently ordered above between-task variability, the external description of a lift—its load, height, and reach—captures only part of the variability in actual spinal exposure, leaving a substantial posture- and person-dependent share unaddressed. Two workers performing the same nominally specified task did not incur the same lumbar loading [44,45]. An assessment aimed at the internal loading environment, as opposed to the external task, will therefore benefit from observing how a load is handled and not only what is handled. This does not diminish the value of task-level descriptors, which remain the dominant drivers of both outcomes; it indicates that they are incomplete on their own.

The most immediate applied-physiology question raised by the cross-classification results is which lifting configurations produce elevated anterior–posterior shear while compression remains below the conventional criterion. A focused validation study should therefore deliberately sample this discordant region by varying load magnitude, horizontal hand location, lower-extremity posture, trunk and pelvic orientation, and asymmetry within a repeated-measures design. Whole-body kinematics, external forces, and trunk-muscle electromyography could then be used to determine which combinations of task geometry and individual movement strategy consistently generate shear-dominant loading. The

subsequent field-validation step would assess how frequently these configurations occur in representative workplaces and whether compression-only screening fails to identify them.

Taken together, these results support a multidimensional view of spinal loading in which compression and shear are evaluated as related but non-equivalent outcomes, each with its own determinants, rather than collapsed into a single index. The present work does not itself constitute such an assessment system, and its conclusions are bounded by the simulated origin of the loading estimates and the finite postural range of the pooled dataset. What it offers is a biomechanically grounded rationale for why a multidimensional framework is warranted, and a demonstration that the determinants distinguishing the two loading components are recoverable from accessible task and posture descriptors. That recoverability is what makes the prospect a practical one: if the distinctions that separate compression from shear can be expressed through measurable posture variables, then posture-aware ergonomic tools—including emerging approaches in computer-vision pose estimation and sparse wearable sensing—may eventually bring this richer picture of spinal loading within reach of routine industrial assessment. Realizing that possibility will require validation against direct loading measurements and testing under field conditions; the contribution of the present study is to establish the mechanistic and statistical grounds on which such efforts can build.

4.6. Limitations and Future Work

Several limitations should be considered when interpreting these findings. First, lumbar compression and shear were estimated from digital human reconstructions rather than measured directly, and the pooled dataset combined lifting conditions from multiple source studies with differences in task context and acquisition procedures. Although participant-specific anthropometric scaling was incorporated in the models, the available covariates do not allow the observed between-subject variability or the fixed sex effect to be partitioned among anthropometry, strength, lifting experience, neuromuscular control, and posture-selection strategy. The sex coefficient should therefore be interpreted as an adjusted group difference rather than as evidence of a specific biological mechanism. Similarly, the present models characterize population-level associations over the finite range of lifting postures represented in the dataset and should not be extrapolated beyond that range without validation. An important next step is to identify experimentally the combinations of load, hand position, trunk and pelvic orientation, lower-extremity posture, asymmetry, and individual lifting strategy that produce elevated shear while compression remains below conventional screening criteria. Controlled physiological studies should then be followed by workplace validation to determine how frequently such compression–shear discordance occurs in occupational lifting and whether multidimensional assessment identifies exposure conditions that compression-only screening overlooks.

5. Conclusions

The present study compared lumbar compression and anterior–posterior shear as paired outcomes estimated from identical lifting data under matched mixed-effects model structures, thereby reducing differences attributable to statistical specification and allowing the outcome-specific patterns to be interpreted in relation to spinal mechanics. Two findings define the result. First, the two loading components share their dominant external drivers—load magnitude and horizontal reach—but separate along interpretable geometric lines in their posture sensitivities: compression tracks the distance at which the supported mass acts from the lumbar spine, whereas shear tracks the orientation of the lumbar segment. Because no predictor significant in both families reversed sign, posture functions as a selective modulator of two independently sourced quantities rather than as a mechanism

that trades one loading component for the other. Second, between-subject variability consistently exceeded between-task variability and persisted across model reduction, indicating that how a load is lifted, beyond the parameters of the task itself, is a structural rather than incidental contributor to spinal exposure.

The observed sex coefficient should be interpreted only as an adjusted group difference within the pooled dataset; although participant-specific anthropometric scaling was incorporated in the digital human models, the analysis did not include separate covariates sufficient to partition that difference among anthropometric, strength-related, experiential, and posture-selection mechanisms or to establish a causal effect of sex.

Together these results provide a quantitative rationale for regarding compression-only assessment as structurally incomplete: a metric anchored to axial compression cannot, by construction, report the shear consequences of a given posture, and the two components are not jointly optimized by a single compression-based guideline. Because the determinants distinguishing them proved recoverable from accessible task and posture descriptors, the framework offers a biomechanically grounded foundation for multidimensional, posture-aware ergonomic tools capable of bringing a richer picture of spinal loading within reach of routine industrial assessment. These conclusions are bounded by the simulated origin of the loading estimates and the finite postural range of the pooled dataset; validation against direct loading measurements and testing under field conditions remain necessary next steps.

Author Contributions: Conceptualization, D.P. and X.J.; methodology, D.P. and X.J.; software, X.J.; validation, D.P. and X.J.; formal analysis, D.P.; investigation, X.J.; resources, D.P.; data curation, X.J.; writing—original draft preparation, D.P.; writing—review and editing, D.P. and X.J.; visualization, D.P.; supervision, D.P.; project administration, D.P.; funding acquisition, D.P. All authors have read and agreed to the published version of the manuscript.

Funding: This research received no external funding.

Informed Consent Statement: This paper used de-identified data from published research.

Data Availability Statement: These data were derived from the following resources available in the public domain.

Acknowledgments: During the preparation of this manuscript, the authors used Grammarly (Version 14.1270.0) for the purposes of finding grammatical mistakes, spelling errors, and typos. The authors have reviewed and edited the output and take full responsibility for the content of this publication.

Conflicts of Interest: The authors declare no conflict of interest.

Appendix A

This appendix contains additional information that complements the regression analyses described in the main text. Table A1 outlines the complete set of biomechanical, anthropometric, and task-specific variables used in the mixed-effects models, including definitions and measurement units. Table A2 provides the fixed- and random-effect estimates for all twelve model formulations, accompanied by their Confidence Intervals. Table A3 compiles the p-values for each predictor across models, with non-significant entries emphasized to assist interpretation. Collectively, these tables give readers a comprehensive overview of the statistical framework employed to model L4/L5 shear forces across different participants, tasks, and experimental protocols.

Table A1. Nomenclature of Variables Included in the Regression Models.

Variable Name	Symbol/Abbreviation	Units	Description
Load	Load_kg	kg	Mass of the lifted object at the moment of exertion.
Horizontal Distance	H_cm	cm	Horizontal reach distance from the midpoint between the ankles to the hands.
Vertical Height	V_cm	cm	Vertical height of the hands at the moment of lift initiation or peak load.
Sex (Male)	Sex_M	(binary)	Participant sex coded as 1 = male, 0 = female.
Coupling Quality	Coupling_Good	(binary)	Quality of hand–object coupling (1 = good grip, 0 = poor).
Hip Flexion Angle	HipFlex_deg	degrees (°)	Angle between the femur and pelvis relative to the neutral standing posture.
Knee Flexion Angle	KneeFlex_deg	degrees (°)	Angle between the tibia and femur; higher values indicate greater knee bend.
Trunk Flexion Angle	TrunkFlex_deg	degrees (°)	Forward flexion of the torso relative to the pelvis.
Shoulder Flexion Angle	ShoulderFlex_deg	degrees (°)	Flexion of the humerus relative to the torso.
Elbow Flexion Angle	ElbowFlex_deg	degrees (°)	Flexion angle of the elbow joint.
Shoulder Abduction/Adduction	Sh_AbdAdd	degrees (°)	Mediolateral displacement of the humerus from the frontal plane.
Study Identifier	StudyID	(categorical)	Identifies the source study for each observation.
Task Identifier	TaskID	(categorical)	Identifies the lifting task condition within each study.
Participant Identifier	SubjectID	(categorical)	Identifies the participant contributing each observation.
L4/L5 Shear Force	L4L5_Shear_N	Newtons (N)	Estimated shear load at the L4/L5 spinal segment
L4/L5 Compressive Force	L4L5_Compressive_N	Newtons (N)	Estimated compressive load at the L4/L5 spinal segment (outcome variable).

Table A2. Regression Coefficients.

Parameter	S0	S2	S4	S9	S10	S11
Intercept	−1320.9 ± 253.1	−1206.6 ± 230.1	−1191.9 ± 197.3	−1251.7 ± 194.53	−1308.2 ± 177.21	−1313.4 ± 170.93
Sex_M	165.64 ± 13.81	184.2 ± 18.68	191.25 ± 15.18	185.94 ± 18.32	182.20 ± 17.12	181.76 ± 17.13
Load_kg	17.928 ± 3.088	19.255 ± 4.023	20.000 ± 3.785	19.750 ± 2.995	19.492 ± 3.018	19.600 ± 2.251
H_cm	27.596 ± 5.645	25.003 ± 5.322	25.589 ± 4.220	26.014 ± 4.705	27.349 ± 4.263	28.047 ± 4.147
V_cm	2.732 ± 0.826	1.759 ± 0.809	1.532 ± 0.775	1.8205 ± 0.764	2.0536 ± 0.711	1.878 ± 0.682
Coupling_Good	−13.526 ± 18.77	−9.782 ± 29.42	−8.348 ± 25.22	—	—	—
TrunkFlex_deg	−0.377 ± 0.701	−0.866 ± 0.844	−0.087 ± 0.687	—	—	—
HipFlex_deg	−6.466 ± 0.801	−5.572 ± 0.814	−5.148 ± 0.788	−5.622 ± 0.786	−5.811 ± 0.748	−5.613 ± 0.736
KneeFlex_deg	4.195 ± 0.737	3.640 ± 0.675	3.393 ± 0.619	3.656 ± 0.667	3.856 ± 0.605	3.907 ± 0.609
ShoulderFlex_deg	−1.040 ± 0.647	0.674 ± 0.665	0.601 ± 0.633	0.482 ± 0.638	—	—
ElbowFlex_deg	−1.678 ± 0.528	−2.070 ± 0.588	−1.743 ± 0.524	−1.882 ± 0.527	−1.773 ± 0.509	−1.798 ± 0.513
Sh_AbdAdd	0.644 ± 0.688	0.322 ± 0.610	0.043 ± 0.601	—	—	—
StudyID_SD	—	—	—	—	—	—
SubjectID_SD	—	43.64	316.71	42.73	39.836	39.606
TaskID_SD	—	16.34	15.87	10.62	10.866	—
Load_slope_SD	—	—	5.7	—	—	—
H_slope_SD	—	—	6.86	—	—	—
Residual_SD	60.13	44.19	24.49	44.196	44.96	45.488

Table A2. *Cont.*

Parameter	C0	C2	C4	C8	C10	C11
Intercept	−4882.00 ± 1087.00	−5356.50 ± 962.98	−5429.80 ± 877.52	−5343.90 ± 865.02	−5119.80 ± 801.35	−5041.80 ± 806.32
Sex_M	669.29 ± 59.29	800.30 ± 87.01	855.03 ± 75.77	800.38 ± 86.92	799.37 ± 86.98	815.91 ± 88.25
Load_kg	93.45 ± 13.26	101.34 ± 28.98	102.78 ± 27.39	105.08 ± 21.47	105.04 ± 21.23	105.00 ± 21.66
H_cm	80.27 ± 24.24	93.82 ± 21.50	99.85 ± 18.82	92.11 ± 19.25	88.06 ± 18.29	80.75 ± 17.66
V_cm	20.32 ± 3.55	14.63 ± 3.43	13.85 ± 3.23	14.72 ± 3.07	14.33 ± 3.01	15.57 ± 2.88
Coupling_Good	−107.36 ± 80.61	−79.46 ± 204.39	−74.39 ± 190.57	—	—	—
TrunkFlex_deg	−12.71 ± 3.01	−10.98 ± 3.27	−6.79 ± 2.84	−10.95 ± 3.27	−11.03 ± 3.26	−10.28 ± 3.25
HipFlex_deg	−20.34 ± 3.44	−13.39 ± 2.80	−12.11 ± 2.69	−13.18 ± 2.79	−12.80 ± 2.73	−12.64 ± 2.73
KneeFlex_deg	6.80 ± 3.17	3.37 ± 2.26	3.32 ± 1.99	3.40 ± 2.26	3.25 ± 2.25	—
ShoulderFlex_deg	−3.69 ± 2.78	4.83 ± 2.28	3.85 ± 2.32	4.87 ± 2.28	5.27 ± 2.22	6.74 ± 2.01
ElbowFlex_deg	−1.97 ± 2.27	−6.14 ± 2.11	−6.30 ± 2.00	−6.20 ± 2.10	−6.91 ± 1.87	−7.09 ± 1.88
Sh_AbdAdd	1.75 ± 2.95	−1.46 ± 1.98	−1.01 ± 2.00	−1.43 ± 1.98	—	—
StudyID_SD	—	—	—	—	—	—
SubjectID_SD	—	233.78	710.81	233.51	234.01	240.17
TaskID_SD	—	140.15	131.69	107.84	106.5	108.91
Load_slope_SD	—	—	21.24	—	—	—
H_slope_SD	—	—	15.43	—	—	—
Residual_SD	258.23	135.88	90.71	135.78	135.2	134.68

Table A3. *p*-Value Comparison. Bolded Values are not Significant.

Variable	S0	S2	S4	S9	S10	S11	C0	C2	C4	C8	C10	C11
Sex_M	<0.001	<0.001	<0.001	<0.001	<0.001	<0.001	<0.001	<0.001	<0.001	<0.001	<0.001	<0.001
Load_kg	<0.001	<0.001	<0.001	<0.001	<0.001	<0.001	<0.001	0.0007	0.0003	<0.001	<0.001	<0.001
H_cm	<0.001	<0.001	<0.001	<0.001	<0.001	<0.001	0.0013	<0.001	<0.001	<0.001	<0.001	<0.001
V_cm	0.0013	0.032	**0.051**	0.019	0.0048	0.007	<0.001	<0.001	<0.001	<0.001	<0.001	<0.001
Coupling (Good)	**0.473**	**0.74**	**0.741**	–	–	–	**0.186**	**0.698**	**0.697**	–	–	–
TrunkFlex_deg	**0.592**	**0.307**	**0.9**	–	–	–	<0.001	0.0011	0.0188	0.0012	0.001	0.0021
HipFlex_deg	<0.001	<0.001	<0.001	<0.001	<0.001	<0.001	<0.001	<0.001	<0.001	<0.001	<0.001	<0.001
KneeFlex_deg	0.0014	<0.001	<0.001	<0.001	<0.001	<0.001	0.0343	**0.14**	**0.0987**	**0.136**	**0.151**	–
ShoulderFlex_deg	**0.111**	**0.313**	**0.345**	**0.451**	–	–	**0.188**	0.0373	**0.1001**	0.0354	0.0194	0.0012
ElbowFlex_deg	0.002	0.00067	0.00124	0.00055	<0.001	<0.001	**0.388**	0.0044	<0.001	0.004	<0.001	<0.001
Sh_AbdAdd	**0.351**	**0.599**	**0.944**	–	–	–	**0.555**	**0.464**	**0.616**	**0.472**	–	–

References

1. Coenen, P.; Kingma, I.; Boot, C.R.; Twisk, J.W.; Bongers, P.M.; van Dieën, J.H. Cumulative Low Back Load at Work as a Risk Factor of Low Back Pain: A Prospective Cohort Study. *J. Occup. Rehabil.* **2013**, *23*, 11–18. [CrossRef] [PubMed]
2. Marras, W.S.; Lavender, S.A.; Leurgans, S.E.; Rajulu, S.L.; Allread, W.G.; Fathallah, F.A.; Ferguson, S.A. The Role of Dynamic Three-Dimensional Trunk Motion in Occupationally-Related Low Back Disorders. The Effects of Workplace Factors, Trunk Position, and Trunk Motion Characteristics on Risk of Injury. *Spine* **1993**, *18*, 617–628. [PubMed]
3. Marras, W.S.; Lavender, S.A.; Leurgans, S.E.; Fathallah, F.A.; Ferguson, S.A.; Allread, W.G.; Rajulu, S.L. Biomechanical Risk Factors for Occupationally Related Low Back Disorders. *Ergonomics* **1995**, *38*, 377–410. [CrossRef] [PubMed]
4. Kumar, S. Theories of Musculoskeletal Injury Causation. *Ergonomics* **2001**, *44*, 17–47. [CrossRef]
5. Munawir, H.; Wulansari, R.E.; Setiawan, E.; Djunaidi, M. Analysis of Work Posture and Manual Material Handling in a Flour Production Process. *Int. J. Emerg. Trends Eng. Res.* **2020**, *8*, 3720–3727. [CrossRef]
6. Kamarudzaman, M.; Zaki, N.E.A.M.; Rahman, M.N.A. Relationship between Manual Material Handling and Musculoskeletal Disorder among Mechanics at Tyre Service Center. *Int. J. Ind. Manag.* **2023**, *17*, 162–167. [CrossRef]
7. Waters, T.R.; Putz-Anderson, V.; Garg, A. *Applications Manual for the Revised Niosh Lifting Equation*; U.S. Department of Health and Human Services, Centers for Disease Control and Prevention, National Institute for Occupational Safety and Health: Cincinnati, OH, USA, 1994.
8. Das, B. Adverse Health Effects and Perceived Musculoskeletal Pain in the Sawmill Workers of West Bengal, India. *Toxicol. Ind. Health* **2023**, *40*, 9–22. [CrossRef] [PubMed]
9. Gallagher, S.; Marras, W.S. Tolerance of the Lumbar Spine to Shear: A Review and Recommended Exposure Limits. *Clin. Biomech.* **2012**, *27*, 973–978. [CrossRef] [PubMed]
10. Punnett, L.; Wegman, D.H. Work-Related Musculoskeletal Disorders: The Epidemiologic Evidence and the Debate. *J. Electromyogr. Kinesiol.* **2004**, *14*, 13–23. [CrossRef] [PubMed]
11. Waters, T.R.; Putz-Anderson, V.; Garg, A.; Fine, L.J. Revised Niosh Equation for the Design and Evaluation of Manual Lifting Tasks. *Ergonomics* **1993**, *36*, 749–776. [CrossRef] [PubMed]

12. Meepradit, P.; Sunee, N.; Chantrasa, R. The Application of Niosh Lifting Equation to Prevent Musculoskeletal Disorder Risks. *J. Biosci. Med.* **2015**, *03*, 39–44.
13. Waters, T.R.; Lu, M.-L.; Piacitelli, L.A.; Werren, D.; Deddens, J.A. Efficacy of the Revised Niosh Lifting Equation to Predict Risk of Low Back Pain Due to Manual Lifting. *J. Occup. Environ. Med.* **2011**, *53*, 1061–1067. [CrossRef] [PubMed]
14. Elfeituri, F.E.; Taboun, S.M. An Evaluation of the Niosh Lifting Equation: A Psychophysical and Biomechanical Investigation. *Int. J. Occup. Saf. Ergon.* **2002**, *8*, 243–258. [CrossRef] [PubMed]
15. Ghezelbash, F.; Shirazi-Adl, A.; Plamondon, A.; Arjmand, N. Comparison of Different Lifting Analysis Tools in Estimating Lower Spinal Loads—Evaluation of Niosh Criterion. *J. Biomech.* **2020**, *112*, 110024. [CrossRef] [PubMed]
16. Russell, S.J.; Winnemuller, L.; Camp, J.E.; Johnson, P.W. Comparing the Results of Five Lifting Analysis Tools. *Appl. Ergon.* **2007**, *38*, 91–97. [CrossRef] [PubMed]
17. Refai, M.I.; Varrecchia, T.; Chini, G.; Ranavolo, A.; Sartori, M. Assessing Low-Back Loading During Lifting Using Personalized Electromyography-Driven Trunk Models and Niosh-Based Risk Levels. *Front. Bioeng. Biotechnol.* **2025**, *13*, 1486931. [CrossRef] [PubMed]
18. Behjati, M.; Arjmand, N. Biomechanical Assessment of the Niosh Lifting Equation in Asymmetric Load-Handling Activities Using a Detailed Musculoskeletal Model. *Hum. Factors* **2019**, *61*, 191–202. [CrossRef] [PubMed]
19. Arjmand, N.; Amini, M.; Shirazi-Adl, A.; Plamondon, A.; Parnianpour, M. Revised Niosh Lifting Equation May Generate Spine Loads Exceeding Recommended Limits. *Int. J. Ind. Ergon.* **2015**, *47*, 1–8. [CrossRef]
20. Norman, R.; Wells, R.; Neumann, P.; Frank, J.W.; Shannon, H.; Kerr, M.; The Ontario Universities Back Pain Study (OUBPS) Group. A Comparison of Peak Vs Cumulative Physical Work Exposure Risk Factors for the Reporting of Low Back Pain in the Automotive Industry. *Clin. Biomech.* **1998**, *13*, 561–573.
21. Davis, K.G.; Marras, W.S.; Waters, T.R. Evaluation of Spinal Loading During Lowering and Lifting. *Clin. Biomech.* **1998**, *13*, 141–152. [CrossRef] [PubMed]
22. Nail-Ulloa, I.; Zabala, M.; Sesek, R.; Chen, H.; Schall, M.C., Jr. Estimating Compressive and Shear Forces at L5-S1: Exploring the Effects of Load Weight, Asymmetry, and Height Using Optical and Inertial Motion Capture Systems. *Sensors* **2024**, *24*, 194124. [CrossRef] [PubMed]
23. Rejeki, Y.S.; Achiraeniwati, E.; As'AD, N.R.; Shakira, M.A.; Vediana, V. *Work Risk Assessment in the Tea Picking with the Key Indicator Method-Awkward Body Postures (Kim-Abp)*; KNE Social Sciences: Dubai, United Arab Emirates, 2022.
24. Eynipour, A.; Arjmand, N.; Dianat, I.; Soltanian, A.R.; Heidarimoghadam, R. Assessing Musculoskeletal Disorder Risks in an Automobile Part Manufacturing Factory: A Comparison Study of Biomechanical and Ergonomic Tools. *Health Scope* **2024**, *13*, 1–13. [CrossRef]
25. Hafez, K.; Jorgensen, M.J.; Amick, R.Z. Comparison of Acgih Lifting Threshold Limit Values to Validated Low Back Disorder Lifting Assessment Methods Outcomes. *Work J. Prev. Assess. Rehabil.* **2023**, *76*, 1047–1060. [CrossRef] [PubMed]
26. Piovesan, D.; Ji, X. A Statistical Framework for Estimating Spinal Compression Risk in Ergonomic Analysis. *Safety* **2026**, *12*, 93. [CrossRef]
27. Piovesan, D.; Ji, X. Lumbar Shear Force Prediction Models for Ergonomic Assessment of Manual Lifting Tasks. *Appl. Sci.* **2026**, *16*, 1414. [CrossRef]
28. Fox, R.R.; Lu, M.-L.; Occhipinti, E.; Jaeger, M. Understanding Outcome Metrics of the Revised Niosh Lifting Equation. *Appl. Ergon.* **2019**, *81*, 102897. [CrossRef] [PubMed]
29. Donisi, L.; Cesarelli, G.; Pisani, N.; Ponsiglione, A.M.; Ricciardi, C.; Capodaglio, E. Wearable Sensors and Artificial Intelligence for Physical Ergonomics: A Systematic Review of Literature. *Diagnostics* **2022**, *12*, 3048. [CrossRef] [PubMed]
30. Ji, X.; Gao, X.; Swierski, E. Evaluating the Accuracy of Virtual Reality in Replicating Real-Life Human Postures and Forces for Injury Risk Assessment. *Sensors* **2024**, *24*, 7049. [CrossRef] [PubMed]
31. Ji, X.; Hettiarachchige, R.O.; Littman, A.L.E.; Lavery, N.L.; Piovesan, D. Prevent Workers from Injuries in the Brewing Company Via Using Digital Human Modelling Technology. *Appl. Sci.* **2023**, *13*, 3593. [CrossRef]
32. Matijevich, E.S.; Volgyesi, P.; Zelik, K.E. A Promising Wearable Solution for the Practical and Accurate Monitoring of Low Back Loading in Manual Material Handling. *Sensors* **2021**, *21*, 340. [CrossRef] [PubMed]
33. Jung, S.; Su, B.; Wang, H.; Lu, L.; Xie, Z.; Xu, X.; Fitts, E.P. A Computer Vision-Based Lifting Task Recognition Method. *Proc. Hum. Factors Ergon. Soc. Annu. Meet.* **2022**, *66*, 1210–1214. [CrossRef]
34. González-Alonso, J.; Martín-Tapia, P.; González-Ortega, D.; Antón-Rodríguez, M.; Díaz-Pernas, F.J.; Martínez-Zarzuela, M. Me-Ward: A Multimodal Ergonomic Analysis Tool for Musculoskeletal Risk Assessment from Inertial and Video Data in Working Places. *Expert Syst. Appl.* **2025**, *278*, 127212. [CrossRef]
35. Lee, C.J.; Lee, J.K. Inertial Motion Capture-Based Wearable Systems for Estimation of Joint Kinetics: A Systematic Review. *Sensors* **2022**, *22*, 2507. [CrossRef] [PubMed]

36. Ji, X.; Hernandez, J.; Schweitzer, E.; Littman, A. The Accuracy of Dynamic Simulation with the Use of Tsb within Jack Siemens Plm Software. In Proceedings of the International Conference on Industrial Engineering and Operations Management, Monterrey, Mexico, 3–5 November 2021.
37. Ji, X.; Littman, A.; Hettiarachchige, R.O.; Piovesan, D. The Effect of Key Anthropometric and Biomechanics Variables Affecting the Lower Back Forces of Healthcare Workers. *Sensors* **2023**, *23*, 658. [CrossRef] [PubMed]
38. Ji, X.; Tiari, S. Posture Evaluation for the Full-Body Dynamic Simulation in Jack Siemens Plm. *Int. J. Hum. Factors Ergon.* **2022**, *9*, 261–281. [CrossRef]
39. Tabasi, A.; Lazzaroni, M.; Brouwer, N.P.; Kingma, I.; van Dijk, W.; de Looze, M.P.; Toxiri, S.; Ortiz, J.; van Dieën, J.H. Optimizing Calibration Procedure to Train a Regression-Based Prediction Model of Actively Generated Lumbar Muscle Moments for Exoskeleton Control. *Sensors* **2021**, *22*, 87. [CrossRef] [PubMed]
40. Marras, W.S.; Granata, K.P.; Davis, K.G.; Allread, W.G.; Jorgensen, M.J. Spine Loading and Probability of Low Back Disorder Risk as a Function of Box Location on a Pallet. *Hum. Factors Ergon. Manuf. Serv. Ind.* **1997**, *7*, 323–336. [CrossRef]
41. Lynn, S.K.; Noffal, G.J. Lower Extremity Biomechanics During a Regular and Counterbalanced Squat. *J. Strength Cond. Res.* **2012**, *26*, 2417–2425. [CrossRef] [PubMed]
42. Granata, K.P.; Marras, W.S. An Emg-Assisted Model of Trunk Loading During Free-Dynamic Lifting. *J. Biomech.* **1995**, *28*, 1309–1317. [CrossRef] [PubMed]
43. Cruz, J.; Aguilar, I.; Yang, J. The Effects of Sex and Handedness on Lumbar Kinetics During Asymmetric Lifting Tasks: A Pilot Study. In Proceedings of the 7th International Digital Human Modeling Symposium Archive, Iowa City, IA, USA, 29–31 August 2022.
44. Allione, F.; Lazzaroni, M.; Gkikakis, A.E.; Di Natali, C.; Monica, L.; Caldwell, D.G.; Ortiz, J. Flexo: A Flexible Passive Exoskeleton Optimized for Reducing Lower Back Strain in Manual Handling Tasks. *Front. Robot. AI* **2025**, *12*, 1687825. [CrossRef] [PubMed]
45. Davidson, J.M.; McKinnon, C.D.; Dickerson, C.R.; Callaghan, J.P. An Assessment of Back and Shoulder Postures in Single-Handed Exertions: Expanding Ergonomic Reaching Guidelines to Consider Lumbar Spine Axial Twist. *IISE Trans. Occup. Ergon. Hum. Factors* **2024**, *12*, 189–202. [CrossRef] [PubMed]

Disclaimer/Publisher's Note: The statements, opinions and data contained in all publications are solely those of the individual author(s) and contributor(s) and not of MDPI and/or the editor(s). MDPI and/or the editor(s) disclaim responsibility for any injury to people or property resulting from any ideas, methods, instructions or products referred to in the content.